applied sciences

MDPI

Article

Continuous Rotor Dynamics of Multi-Disc and Multi-Span Rotor: A Theoretical and Numerical Investigation on the Identification of Bearing Coefficients from Unbalance Responses

Aiming Wang [1,*], Yujie Bi [2], Xiaohan Cheng [1], Jie Yang [1], Guoying Meng [1], Yun Xia [1] and Yu Feng [1]

[1] School of Mechanical Electronic & Information Engineering, China University of Mining & Technology (Beijing), Beijing 100083, China; chengxh@cumtb.edu.cn (X.C.); 201702@cumtb.edu.cn (J.Y.); mgy@cumtb.edu.cn (G.M.); xiayun@cumtb.edu.cn (Y.X.); fengyu20062009@163.com (Y.F.)

[2] School of Mechanics and Civil Engineering, China University of Mining & Technology (Beijing), Beijing 100083, China; byjpengqiao@126.com

* Correspondence: wam_master@163.com; Tel.: +86-134-8871-3431

Citation: Wang, A.; Bi, Y.; Cheng, X.; Yang, J.; Meng, G.; Xia, Y.; Feng, Y. Continuous Rotor Dynamics of Multi-Disc and Multi-Span Rotor: A Theoretical and Numerical Investigation on the Identification of Bearing Coefficients from Unbalance Responses. *Appl. Sci.* **2022**, *12*, 4251. https://doi.org/10.3390/app12094251

Academic Editors: Jan Awrejcewicz, José A. Tenreiro Machado, José M. Vega, Hari Mohan Srivastava, Ying-Cheng Lai, Hamed Farokhi and Roman Starosta

Received: 17 March 2022
Accepted: 20 April 2022
Published: 22 April 2022

Abstract: Identification of bearings' stiffness and damping coefficients, which strongly affects the dynamic characteristics of rotors, is another inverse problem of Rotor Dynamics. In this paper, aiming at multi-disc and multi-span rotors, two novel algorithms are proposed for identifying each bearing's coefficients based on the continuous rotor dynamic analysis method. A linear functional relationship between the main complex coefficients and the cross-coupled complex coefficients is obtained, which eliminates the coupling between the coefficients and the rotor unbalance in the forward problem. Then, Algorithm I is proposed. However, it is only suitable for rolling-bearing. To solve the problem, changing the rotating speed slightly is proposed to solve the difficulty that another set of equations cannot be developed because the slope of the proposed linear function is constant when the rotating speed is maintained at a fixed speed. Then, Algorithm II, which can be applied to both rolling-bearing and oil-journal bearing, is provided. Numerical investigations are conducted to study the two methods. It is indicated that there should be a measuring point, called an adjustment point, near each bearing, whose coefficients should be identified, to obtain high identification accuracy. Moreover, the identification accuracy of the two algorithms is strongly related to sensor resolution. When the measuring errors of all the required unbalance responses are zero or the same, the identification errors are almost equal to zero. In conclusion, the proposed algorithms provide a method for monitoring the stiffness and damping coefficients of all bearings in a multi-disc and multi-span rotor under operation conditions to predict rotor dynamic behavior for the safe and steady running of rotating machines.

Keywords: identification of bearing stiffness and damping coefficients; inverse problem; rotor dynamics; multi-disc and multi-span rotor

1. Introduction

1.1. Background and Formulation of the Problem

The vibration characteristics of the rotor-bearing system (typically regarded as the main element of rotating machines) are strongly affected by the stiffness and damping coefficients of bearings [1,2]. Bearing coefficients are related to installation, operation and maintenance conditions. Hence, the actual value of bearing coefficients at running status is quite different from the value at the design stage, which results in inconsistency between the operating condition and the design condition. Sometimes it even leads to the failure of large rotating machinery after a trial operation or running for a period of time. Owing to a lack of information on the actual stiffness and damping coefficients of bearings under working conditions, rotor dynamic behavior cannot be predicted accurately for the safe and steady running of rotating machines. In view of these, the identification of bearing coefficients has been an active area of research.

1.2. Literature Survey

Identification of bearing coefficients in a rotor-bearing system is an old problem. Some scholars have investigated theoretical model-based methods to obtain the bearing stiffness and damping coefficients. Snyder [3] tried to predict dynamic coefficients of sliding bearings based on the Reynolds equation and Computational Fluid Dynamics. Li [4] calculated stiffness and damping coefficients of journal bearing using a 3D transient flow calculation. Dyk [5] obtained bearing coefficients based on the approximate analytical solutions of the Reynolds equation. Merelli [6] evaluated the dynamic coefficients of finite length journal bearing using a regular perturbation method. However, the simplification in modeling inevitably leads to errors between the calculated and actual values [7].

Therefore, experimental identification methods were developed. They can be categorized according to the applied load (static load and dynamic force, i.e., using exciter, impulse, or unbalanced force) [8–10]. The static load approach is sensitive to measuring errors, and the methods using an exciter or an impact hammer are not easy to carry out and are time-consuming. From the perspective of practicality, it is easier to apply an unbalanced force than an excitation force because no sophisticated device is required. Hagg and Sankey [11] measured for the first time the journal-bearing coefficients by using an unbalanced force; however, they ignored the cross-coupled stiffness and damping coefficients. Duffin and Johnson [12] used the aforementioned method and proposed an iterative procedure to calculate coefficients including the cross-coupled coefficients of large journal bearings. With the assumption that the excitation frequency does not influence bearing coefficients. Tiwari [13] developed an estimation algorithm using the unbalance responses from bearing housings in the horizontal and vertical directions with the assumption that bearing coefficients are speed dependent. At least two run-downs with different unbalance configurations are obtained. The method has considerable potential because the synchronous responses of rotating machines from a machine run-down/run-up are not difficult to obtain.

Additionally, optimization techniques were investigated. The Bayesian inference optimization technique combined with the imbalance excitation methods was proposed to improve the identification accuracy [14]. However, this method may involve an ill-conditioned matrix problem. To avoid the problem, Chen [15] proposed four complementary equations that are uncorrelated with the dynamic equations from unbalance responses. The least-squares method is combined with vibration theory by Song [16] for estimating the dynamic characteristics of journal bearings.

Some scholars tried to estimate bearing coefficients and rotor unbalance simultaneously [17]. Bently and Muszynska applied different frequency excitations to estimate rotor unbalance as well as bearing coefficients [18]. Based on the method proposed by Stanway [19], Hiroshi Iida [20] conducted an experiment that applied impulse excitation on a double-disc and single-span rotor to identify rotor unbalance as well as stiffness and damping coefficients. Tiwari [21] developed an algorithm to simultaneously estimate rotor unbalance, and four stiffness coefficients and four damping coefficients of bearings in a multi-degree-of-freedom (MDOF) flexible rotor using impulse responses transformed as frequencies. The rotor is modeled as a Timoshenko beam with gyroscopic effects using the finite element method. Standard condensation is utilized to reduce the model's degree of freedom. The algorithm can incorporate any type and any number of bearings. Tiwari [22] subsequently formulated another algorithm for the simultaneous estimation method using unbalance responses from three different unbalance configurations for both clockwise and anti-clockwise rotations. Recently, Tiwari [17] proposed an algorithm for flexible rotors for the simultaneous estimation of bearing coefficients and rotor unbalance from run-down responses. In the estimation, ill-conditioning occurred because of considerable differences among the parameter values. To resolve this, Tikhonov regularization was employed. The above methods require an exciter and are difficult to implement. In the case of large rotors, high-power exciters, which may damage rotors, are necessary.

Few scholars have investigated the simultaneous estimation methods that do not require external excitation. Tiwari [23] developed a method for the estimation of rotor unbalance and bearing coefficients for MDOF rotors simultaneously. The unbalance responses of the rotor, which alternately rotates clockwise and anti-clockwise, are employed to resolve the ill-conditioning of the regression matrix. Wang [24] proposed a simultaneous estimation of bearing coefficients and rotor unbalance of continuous single-disc and single-span rotors using the Rayleigh beam model. However, the methods do not incorporate any number of bearings and discs.

1.3. Scope and Contribution of This Study

In the present paper, two novel algorithms are proposed to identify all bearings' coefficients of multi-disc and multi-span rotor with m discs and n bearings from unbalance responses based on the continuous rotor dynamic analysis method (CRDAM). The matrix method is proposed to overcome the difficulties that equations of the inverse problem are non-linear transcendental, too many unknown variables are included in the equations and rotor unbalances and bearing coefficients are coupling together. Then, a linear function, which represents the relationship between the main complex coefficients and the cross-coupled complex coefficients, is proposed to obtain Algorithm I. However, the algorithm can only be applied to identifying the main stiffness and damping coefficients of rolling-bearing, of which the cross-coupled coefficients can be considered zero. To identify the cross-coupled coefficients together with the main coefficients, there is a difficulty that another set of equations cannot be easily developed based on the proposed function just by using doubled unbalance responses as input. The reason is the slope of the proposed linear function is constant when the rotating speed is maintained at a fixed speed. Changing the rotating speed slightly is proposed to obtain another equation set and Algorithm II is provided for estimating all the eight coefficients of a bearing. Algorithm II is suitable for the identification of coefficients of both rolling bearings and journal bearings in a rotor. The number of required measuring points of unbalance responses is m + n + 1. Three kinds of numerical simulations are conducted to validate the two algorithms. It is indicated that the two algorithms have high identification accuracy when the measurement errors of all input unbalance responses are zero or the same. There should be a measuring point, called an adjustment point, to achieve high identification accuracy. The adjustment point should be near the bearing, whose coefficients are to be identified. The proposed algorithms do not require a machine run-down/run-up and external exciters, and have the flexibility to incorporate any number of bearings and discs.

1.4. Organization of the Paper

The remainder of this paper is organized as follows. Section 2 discusses the modeling of the proposed algorithms based on CRDAM. Section 3 describes the numerical investigations for examining the algorithms. Section 4 summarizes the conclusions of the study.

2. Theory

2.1. Algorithm I for Identification of Main Stiffness and Damping Coefficients of Rolling Bearings

Aiming at a rotor with m discs and n bearings shown in Figure 1, the continuous rotor dynamic analysis method (CRDAM) is proposed in reference [25]. Based on CRDAM, the unbalance response can be expressed as the function of the position, rotor unbalances, the bearings' stiffness and damping coefficients. Accordingly, the inverse problem, which is identifying rotor unbalances, is solved in reference [26]. The matrix method is proposed to solve the problems that: the equations built based on CRDAM are non-linear transcendental, there are too many unknown variables in the equations, and the rotor unbalances and bearings' coefficients are coupling together. The following equations, which eliminate the coupling between the coefficients and the rotor unbalances, are proposed in reference [26].

$$\begin{bmatrix} \pi \cdot w^2 \cdot m_{1u} e_1 \cdot (\sin\alpha_1 - i \cdot \cos\alpha_1) + L \cdot w^2 \cdot m_{1d} U_{1d} \\ \vdots \\ \pi \cdot w^2 \cdot m_{mu} e_m \cdot (\sin\alpha_m - i \cdot \cos\alpha_m) + L \cdot w^2 \cdot m_{md} U_{md} \\ -L \cdot k_{1s \cdot yx} \cdot V_{1b} - L \cdot k_{1s \cdot yy} \cdot U_{1b} \\ \vdots \\ -L \cdot k_{ns \cdot yx} \cdot V_{nb} - L \cdot k_{ns \cdot yy} \cdot U_{nb} \end{bmatrix}_{m+n} = \frac{EI}{L^2} \cdot H_1{}^{-1} \begin{bmatrix} U(q_{1s}) \\ \vdots \\ U(q_{ms}) \\ U\left(q_{(m+1)s}\right) \\ \vdots \\ U\left(q_{(m+n)s}\right) \end{bmatrix} = H_2 \tag{1}$$

$$\begin{bmatrix} \pi \cdot w^2 \cdot m_{u1} \cdot e_1 \cdot (\cos\alpha_1 + i \cdot \sin\alpha_1) + w^2 \cdot m_{1d} L \cdot V_{1d} \\ \vdots \\ \pi \cdot w^2 \cdot m_{mu} \cdot e_m \cdot (\cos\alpha_m + i \cdot \sin\alpha_m) + w^2 \cdot m_{md} L \cdot V_{md} \\ -L \cdot k_{1s \cdot xy} U_{1b} - L \cdot k_{1s \cdot xx} V_{1b} \\ \vdots \\ -L \cdot k_{ns \cdot xy} U_{nb} - L \cdot k_{ns \cdot xx} V_{nb} \end{bmatrix}_{m+n} = \frac{EI}{L^2} \cdot H_3{}^{-1} \begin{bmatrix} V(q_{1s}) \\ \vdots \\ V(q_{ms}) \\ V\left(q_{(m+1)s}\right) \\ \vdots \\ V(q_{ns}) \end{bmatrix} = H_4 \tag{2}$$

where w is the rotation frequency; L is the length of the shaft; E is the elastic modulus of the shaft; I is the diametric shaft cross-sectional geometric moment of inertia; $m_{1u} \cdots m_{mu}$ are the eccentric masses of #1 $\cdots m$ disc; $e_1 \cdots e_m$ are the eccentric distance of #1 $\cdots m$ disc; $\alpha_1 \cdots \alpha_m$ are the eccentric angles, which are defined as the angles between the x-axis and the disc's eccentric position in the rotation direction; $m_{1d} \cdots m_{md}$ are the masses of #1 $\cdots m$ disc; $U_{1d} \cdots U_{md}$ represent the dimensionless unbalance response of each disc in the frequency domain in the y direction; $V_{1d} \cdots V_{md}$ represent the dimensionless unbalance response of each disc in the frequency domain in the x direction; $U_{1b} \cdots U_{nb}$ represent the dimensionless unbalance response of each bearing in the frequency domain in the y direction; $V_{1b} \cdots V_{nb}$ represent the dimensionless unbalance response of each bearing in the frequency domain in the x direction. $q_{1s}, \ldots, q_{ms}$ and $q_{(m+1)s}, \ldots, q_{(m+n)s}$ are their dimensionless values of locations on the shaft excluding locations of all discs and bearings; $U(q_{1s}), \ldots, U(q_{ms})$ and $U\left(q_{(m+1)s}\right), \ldots, U\left(q_{(m+n)s}\right)$ are the measured dimensionless unbalance responses in the frequency domain in the y direction of locations excluding all discs and bearings; $V(q_{1s}), \ldots, V(q_{ms})$ and $V\left(q_{(m+1)s}\right), \ldots, V\left(q_{(m+n)s}\right)$ are the measured dimensionless unbalance responses in the frequency domain in the y direction of locations excluding all discs and bearings; $k_{1s \cdot xx}, k_{1s \cdot yy}, \ldots, k_{ns \cdot xx}, k_{ns \cdot yy}$ are the main complex coefficients; $k_{1s \cdot xy}$, $k_{1s \cdot yx}, \ldots, k_{ns \cdot xy}, k_{ns \cdot yx}$ are the cross-coupled complex coefficients defined in Equation (3); H_1 and H_3 are the $(m+n) \times (m+n)$ matrices defined in Equations (4) and (5) and can be calculated using Green's functions $G_u(q, q_i)$ and $G_v(q, q_i)$ as long as the locations of the measuring points, the bearings and the discs are known; $q = z/L$; z is the axial position of the shaft; q_i is the dimensionless location of the bearings and discs.

$$\begin{cases} k_{1s \cdot xx} = k_{1 \cdot xx} + i \cdot w \cdot c_{1 \cdot xx} \\ k_{1s \cdot xy} = k_{1 \cdot xy} + i \cdot w \cdot c_{1 \cdot xy} \\ k_{1s \cdot yy} = k_{1 \cdot yy} + i \cdot w \cdot c_{1 \cdot yy} \\ k_{1s \cdot yx} = k_{1 \cdot yx} + i \cdot w \cdot c_{1 \cdot yx} \end{cases}, \quad \ldots, \quad \begin{cases} k_{ns \cdot xx} = k_{n \cdot xx} + i \cdot w \cdot c_{n \cdot xx} \\ k_{ns \cdot xy} = k_{n \cdot xy} + i \cdot w \cdot c_{n \cdot xy} \\ k_{ns \cdot yy} = k_{n \cdot yy} + i \cdot w \cdot c_{n \cdot yy} \\ k_{ns \cdot yx} = k_{n \cdot yx} + i \cdot w \cdot c_{n \cdot yx} \end{cases} \tag{3}$$

$$H_1 = \begin{bmatrix} G_u(q_{1s}, q_{1d}) & \cdots & G_u(q_{1s}, q_{md}) & G_u(q_{1s}, q_{1b}) & \cdots & G_u(q_{1s}, q_{nb}) \\ \vdots & \vdots & \vdots & \vdots & \vdots & \vdots \\ G_u(q_{ms}, q_{1d}) & \cdots & G_u(q_{ms}, q_{md}) & G_u(q_{ms}, q_{1b}) & \cdots & G_u(q_{ms}, q_{nb}) \\ G_u\left(q_{(m+1)s}, q_{1d}\right) & \cdots & G_u\left(q_{(m+1)s}, q_{md}\right) & G_u\left(q_{(m+1)s}, q_{1b}\right) & \cdots & G_u\left(q_{(m+1)s}, q_{nb}\right) \\ \vdots & \cdots & \vdots & \vdots & \cdots & \vdots \\ G_u\left(q_{(m+n)s}, q_{1d}\right) & \cdots & G_u\left(q_{(m+n)s}, q_{md}\right) & G_u\left(q_{(m+n)s}, q_{1b}\right) & \cdots & G_u\left(q_{(m+n)s}, q_{nb}\right) \end{bmatrix}_{(m+n)\times(m+n)} \quad (4)$$

$$H_3 = \begin{bmatrix} G_v(q_{1s}, q_{1d}) & \cdots & G_v(q_{1s}, q_{md}) & G_v(q_{1s}, q_{1b}) & \cdots & G_v(q_{1s}, q_{nb}) \\ G_v(q_{ms}, q_{1d}) & & G_v(q_{ms}, q_{md}) & G_v(q_{ms}, q_{1b}) & & G_v(q_{ms}, q_{nb}) \\ G_v\left(q_{(m+1)s}, q_{1d}\right) & & G_v\left(q_{(m+1)s}, q_{md}\right) & G_v\left(q_{(m+1)s}, q_{1b}\right) & & G_v\left(q_{(m+1)s}, q_{nb}\right) \\ G_v(q_{ns}, q_{1d}) & & G_v(q_{ns}, q_{md}) & G_v(q_{ns}, q_{1b}) & & G_v(q_{ns}, q_{nb}) \end{bmatrix}_{(m+n)\times(m+n)} \quad (5)$$

where $q_{1d} = z_{1d}/L, \cdots, q_{md} = z_{md}/L$, $q_{1b} = z_{1b}/L, \cdots, q_{nb} = z_{nb}/L$; $z_{1d}, \cdots, z_{md}$ are the z coordinate positions of each disc; $z_{1b}, \cdots z_{nb}$ are the z coordinate positions of each bearing; $G_u(q, q_{1d}), \cdots, G_u(q, q_{md})$, $G_u(q, q_{1b}), \cdots, G_u(q, q_{nb})$, $G_v(q, q_{1d}), \cdots, G_v(q, q_{md})$, $G_v(q, q_{1b}), \cdots, G_v(q, q_{nb})$ are Green's coefficients, which can be calculated using Green's functions; Green's functions $G_u(q, q_i)$ and $G_v(q, q_i)$ can be found in reference [24].

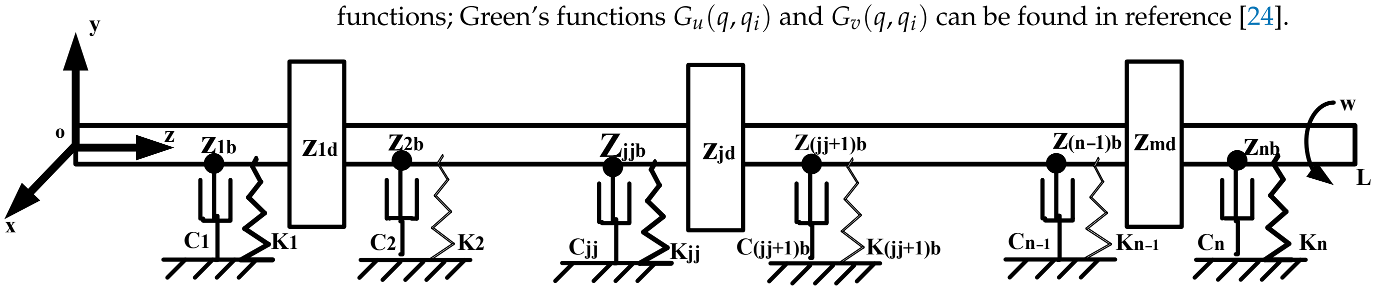

Figure 1. Multi-disc and multi-span rotor-bearing system.

According to Equation (1), Equation (6) can be obtained.

$$\begin{cases} -L \cdot k_{1s\cdot yx} \cdot V_{1b} - L \cdot k_{1s\cdot yy} \cdot U_{1b} = H_2(m+1, 1) \\ \vdots \\ -L \cdot k_{ns\cdot yx} \cdot V_{nb} - L \cdot k_{ns\cdot yy} \cdot U_{nb} = H_2(m+n, 1) \end{cases} \quad (6)$$

Write Equation (6) in another form and the linear functional relationship between the main complex coefficients and the cross-coupled complex coefficients in the y direction can be proposed in Equation (7).

$$\begin{cases} k_{1s\cdot yx} + k_{1s\cdot yy} \cdot \frac{U_{1b}}{V_{1b}} = \frac{-H_2(m+1,1)}{L\cdot V_{1b}} \\ \vdots \\ k_{ns\cdot yx} + k_{ns\cdot yy} \cdot \frac{U_{nb}}{V_{nb}} = \frac{-H_2(m+n,1)}{L\cdot V_{nb}} \end{cases} \quad (7)$$

For rolling bearings, the cross-coupled stiffness coefficient and the cross-coupled damping coefficient in the y direction can be considered zero. $k_{1s\cdot yx} = \cdots = k_{ns\cdot yx} = 0$. Hence, Equation (8) can be obtained according to Equation (7).

$$\begin{cases} k_{1s\cdot yy} = \frac{H_2(m+1,1)}{-L\cdot U_{1b}} \\ \vdots \\ k_{ns\cdot yy} = \frac{H_2(m+n,1)}{-L\cdot U_{nb}} \end{cases} \quad (8)$$

Therefore, the main stiffness coefficients and main damping coefficients in the y direction can be calculated based on Equation (8). In the formula, the matrix H_2 can be calculated using m + n unbalance responses in the y direction, and the unbalance response of the bearing, whose coefficients are to be estimated, must be measured. Hence, the total number of input unbalance responses in the y direction is m + n + 1. To identify all the bearings' coefficients simultaneously, the unbalance responses of all the bearings in the y direction are required.

Similarly, Equation (9) can be obtained according to Equation (2) in the x direction.

$$\begin{cases} -L \cdot k_{1s \cdot xy} U_{1b} - L \cdot k_{1s \cdot xx} V_{1b} = H_4(m+1,1) \\ \vdots \\ -L \cdot k_{ns \cdot xy} U_{nb} - L \cdot k_{ns \cdot xx} V_{nb} = H_4(n,1) \end{cases} \tag{9}$$

According to Equation (9), the linear functional relationship between the main complex coefficients and the cross-coupled complex coefficients in the x direction can be obtained in Equation (10).

$$\begin{cases} k_{1s \cdot xy} + k_{1s \cdot xx} \cdot \frac{V_{1b}}{U_{1b}} = \frac{H_4(m+1,1)}{-L \cdot U_{1b}} \\ \vdots \\ k_{ns \cdot xy} + k_{ns \cdot xx} \cdot \frac{V_{nb}}{U_{nb}} = \frac{H_4(n,1)}{-L \cdot U_{nb}} \end{cases} \tag{10}$$

For rolling bearings, the cross-coupled stiffness coefficient and the cross-coupled damping coefficient in the x direction can be considered zero. $k_{1s \cdot xy} = \cdots = k_{ns \cdot xy} = 0$. Hence, Equation (11) can be obtained according to Equation (10).

$$\begin{cases} k_{1s \cdot xx} = \frac{H_4(m+1,1)}{-L \cdot V_{1b}} \\ \vdots \\ k_{ns \cdot xx} = \frac{H_4(n,1)}{-L \cdot V_{nb}} \end{cases} \tag{11}$$

Hence, the main coefficients in the x direction can be calculated based on Equation (11). In the formula, the matrix H_4 be calculated using m + n unbalance responses in the x direction and the unbalance response of the bearing, whose coefficients are to be estimated, must be measured. Hence, the total number of input unbalance responses in the x direction is m + n + 1. To identify all the bearings' coefficients simultaneously, the unbalance responses of all the bearings in the x direction should be measured.

2.2. Algorithm II for Identification of Bearings' Main and Cross-Coupled Coefficients

Although the algorithm provided by Equations (8) and (11) is suitable to identify the main stiffness and damping coefficients of each bearing in a rolling-bearing rotor with m discs and n bearings, it cannot be used for estimating both the main and the cross-coupled coefficients of journal bearings. The reason is that the cross-coupled stiffness and damping coefficients of journal bearings are very big and cannot be ignored. Another set of equations is required in this case. However, the second equation set cannot be simply built just by adding more measuring unbalance responses because the slop U_{nb}/V_{nb} can be proved constant for a single-span and single-disc rotor when the rotating speed is maintained at a fixed speed [27]. Moreover, using double measuring points can make the measuring system complex and costly.

Although the values of the stiffness and damping coefficients change with the rotating speed, the changing relationship is extremely gradual. Hence, the bearing coefficients can be considered unchangeable when the rotating speed is slightly modified. By slightly changing the rotating speed from w to w', the second set of Equations (12) and (13) are obtained according to Equations (7) and (10).

$$\begin{cases} k_{1s\cdot yx} + k_{1s\cdot yy} \cdot \frac{U_{1b}'}{V_{1b}'} = \frac{-H_2'(m+1,1)}{L\cdot V_{1b}'} \\ \vdots \\ k_{ns\cdot yx} + k_{ns\cdot yy} \cdot \frac{U_{nb}'}{V_{nb}'} = \frac{-H_2'(n+1,1)}{L\cdot V_{nb}'} \end{cases} \tag{12}$$

$$\begin{cases} k_{1s\cdot xy} + k_{1s\cdot xx} \cdot \frac{V_{1b}'}{U_{1b}'} = \frac{H_4'(m+1,1)}{-L\cdot U_{1b}'} \\ \vdots \\ k_{ns\cdot xy} + k_{ns\cdot xx} \cdot \frac{V_{1b}'}{U_{1b}'} = \frac{H_4'(n,1)}{-L\cdot U_{nb}'} \end{cases} \tag{13}$$

where $U_{1b}', U_{2b}', \ldots, U_{nb}'$ represent the dimensionless unbalance responses of each bearing in the frequency domain in the y direction when the rotating frequency is changed to ω'; $V_{1b}', V_{2b}', \ldots, V_{nb}'$ represent the dimensionless unbalance responses of each bearing in the frequency domain in the x direction when the rotating frequency is changed to ω'. H_2' and H_4' can also be calculated based on CRDAM using the m + n measuring unbalance responses when the rotating frequency is changed to ω'.

By expanding the complex coefficients in Equations (12) and (13) to form the imaginary part and real part, the following can be obtained

$$\begin{array}{c} \begin{cases} k_{1\cdot yx} + i\cdot w\cdot c_{1\cdot yx} + (k_{1\cdot yy} + i\cdot w\cdot c_{1\cdot yy})\cdot \frac{U_{1b}}{V_{1b}} = \frac{-H_2(m+1,1)}{L\cdot V_{1b}} \\ k_{1\cdot yx} + i\cdot w'\cdot c_{1\cdot yx} + (k_{1\cdot yy} + i\cdot w'\cdot c_{1\cdot yy})\cdot \frac{U_{1b}'}{V_{1b}'} = \frac{-H_2'(m+1,1)}{L\cdot V_{1b}'} \end{cases} \\ \vdots \\ \begin{cases} k_{n\cdot yx} + i\cdot w\cdot c_{n\cdot yx} + (k_{n\cdot yy} + i\cdot w\cdot c_{n\cdot yy})\cdot \frac{U_{nb}}{V_{nb}} = \frac{-H_2(n+1,1)}{L\cdot V_{nb}} \\ k_{n\cdot yx} + i\cdot w'\cdot c_{n\cdot yx} + (k_{n\cdot yy} + i\cdot w'\cdot c_{n\cdot yy})\cdot \frac{U_{nb}'}{V_{nb}'} = \frac{-H_2'(n+1,1)}{L\cdot V_{nb}'} \end{cases} \end{array} \tag{14}$$

$$\begin{array}{c} \begin{cases} k_{1\cdot xy} + i\cdot w\cdot c_{1\cdot xy} + (k_{1\cdot xx} + i\cdot w\cdot c_{1\cdot xx})\cdot \frac{V_{1b}}{U_{1b}} = \frac{H_4(m+1,1)}{-L\cdot U_{1b}} \\ k_{1\cdot xy} + i\cdot w'\cdot c_{1\cdot xy} + (k_{1\cdot xx} + i\cdot w'\cdot c_{1\cdot xx})\cdot \frac{V_{1b}'}{U_{1b}'} = \frac{H_4(m+1,1)}{-L\cdot U_{1b}'} \end{cases} \\ \vdots \\ \begin{cases} k_{n\cdot xy} + i\cdot w\cdot c_{n\cdot xy} + (k_{n\cdot xx} + i\cdot w\cdot c_{n\cdot xx})\cdot \frac{V_{nb}}{U_{nb}} = \frac{H_4(n,1)}{-L\cdot U_{nb}} \\ k_{n\cdot xy} + i\cdot w'\cdot c_{n\cdot xy} + (k_{n\cdot xx} + i\cdot w'\cdot c_{n\cdot xx})\cdot \frac{V_{nb}'}{U_{nb}'} = \frac{H_4(n,1)}{-L\cdot U_{nb}} \end{cases} \end{array} \tag{15}$$

Therefore, according to Equation (14), Equation (16) is obtained. It can be used to calculate the stiffness and damping coefficients of each bearing in the y direction. According to Equation (15), Equation (17), which can be used for estimating the coefficients of each bearing in the x direction, is obtained. According to Equations (16) and (17), there should be m + n unbalance responses in both x and y directions to obtain the matrices H_2, H_2', H_4 and H_4'. If a bearing's coefficients should be identified, its unbalance responses in both x and y directions are required. Hence, there should be m + n + 1 measured unbalance responses in the two orthogonal directions. To identify all the bearings' coefficients, the unbalance responses of all bearings must be measured.

$$
\begin{aligned}
&\begin{bmatrix} k_{1\cdot yy} \\ k_{1\cdot yx} \\ c_{1\cdot yy} \\ c_{1\cdot yx} \end{bmatrix} = \begin{bmatrix} Re\left(\frac{U_{1b}}{V_{1b}}\right) & 1 & w\cdot Im\left(\frac{U_{1b}}{V_{1b}}\right) & 0 \\ Im\left(\frac{U_{1b}}{V_{1b}}\right) & 0 & w\cdot Re\left(\frac{U_{1b}}{V_{1b}}\right) & w \\ Re\left(\frac{U_{1b}{}'}{V_{1b}{}'}\right) & 1 & w'\cdot Im\left(\frac{U_{1b}{}'}{V_{1b}{}'}\right) & 0 \\ Im\left(\frac{U_{1b}{}'}{V_{1b}{}'}\right) & 0 & w'\cdot Re\left(\frac{U_{1b}{}'}{V_{1b}{}'}\right) & w' \end{bmatrix}^{-1} \cdot \begin{bmatrix} Re\left(\frac{-H_2(m+1,1)}{L\cdot V_{1b}}\right) \\ Im\left(\frac{-H_2(m+1,1)}{L\cdot V_{1b}}\right) \\ Re\left(\frac{-H_2{}'(m+1,1)}{L\cdot V_{1b}{}'}\right) \\ Im\left(\frac{-H_2{}'(m+1,1)}{L\cdot V_{1b}{}'}\right) \end{bmatrix} \\
&\qquad\vdots \\
&\begin{bmatrix} k_{n\cdot yy} \\ k_{n\cdot yx} \\ c_{n\cdot yy} \\ c_{n\cdot yx} \end{bmatrix} = \begin{bmatrix} Re\left(\frac{U_{nb}}{V_{nb}}\right) & 1 & w\cdot Im\left(\frac{U_{nb}}{V_{nb}}\right) & 0 \\ Im\left(\frac{U_{nb}}{V_{nb}}\right) & 0 & w\cdot Re\left(\frac{U_{nb}}{V_{nb}}\right) & w \\ Re\left(\frac{U_{nb}{}'}{V_{nb}{}'}\right) & 1 & w'\cdot Im\left(\frac{U_{nb}{}'}{V_{nb}{}'}\right) & 0 \\ Im\left(\frac{U_{nb}{}'}{V_{nb}{}'}\right) & 0 & w'\cdot Re\left(\frac{U_{nb}{}'}{V_{nb}{}'}\right) & w' \end{bmatrix}^{-1} \cdot \begin{bmatrix} Re\left(\frac{-H_2(n,1)}{L\cdot V_{nb}}\right) \\ Im\left(\frac{-H_2(n,1)}{L\cdot V_{nb}}\right) \\ Re\left(\frac{-H_2{}'(n,1)}{L\cdot V_{nb}{}'}\right) \\ Im\left(\frac{-H_2{}'(n,1)}{L\cdot V_{nb}{}'}\right) \end{bmatrix}
\end{aligned}
\tag{16}
$$

$$
\begin{aligned}
&\begin{bmatrix} k_{1\cdot xx} \\ k_{1\cdot xy} \\ c_{1\cdot xx} \\ c_{1\cdot xy} \end{bmatrix} = \begin{bmatrix} Re\left(\frac{V_{1b}}{U_{1b}}\right) & 1 & w\cdot Im\left(\frac{V_{1b}}{U_{1b}}\right) & 0 \\ Im\left(\frac{V_{1b}}{U_{1b}}\right) & 0 & w\cdot Re\left(\frac{V_{1b}}{U_{1b}}\right) & w \\ Re\left(\frac{V_{1b}{}'}{U_{1b}{}'}\right) & 1 & w'\cdot Im\left(\frac{V_{1b}{}'}{U_{1b}{}'}\right) & 0 \\ Im\left(\frac{V_{1b}{}'}{U_{1b}{}'}\right) & 0 & w'\cdot Re\left(\frac{V_{1b}{}'}{U_{1b}{}'}\right) & w' \end{bmatrix}^{-1} \cdot \begin{bmatrix} Re\left(\frac{H_4(m+1,1)}{-L\cdot U_{1b}}\right) \\ Im\left(\frac{H_4(m+1,1)}{-L\cdot U_{1b}}\right) \\ Re\left(\frac{H_4{}'(m+1,1)}{-L\cdot U_{1b}{}'}\right) \\ Im\left(\frac{H_4{}'(m+1,1)}{-L\cdot U_{1b}{}'}\right) \end{bmatrix} \\
&\qquad\vdots \\
&\begin{bmatrix} k_{n\cdot xx} \\ k_{n\cdot xy} \\ c_{n\cdot xx} \\ c_{n\cdot xy} \end{bmatrix} = \begin{bmatrix} Re\left(\frac{V_{nb}}{U_{nb}}\right) & 1 & w\cdot Im\left(\frac{V_{nb}}{U_{nb}}\right) & 0 \\ Im\left(\frac{V_{nb}}{U_{nb}}\right) & 0 & w\cdot Re\left(\frac{V_{nb}}{U_{nb}}\right) & w \\ Re\left(\frac{V_{nb}{}'}{U_{nb}{}'}\right) & 1 & w'\cdot Im\left(\frac{V_{nb}{}'}{U_{nb}{}'}\right) & 0 \\ Im\left(\frac{V_{nb}{}'}{U_{nb}{}'}\right) & 0 & w'\cdot Re\left(\frac{V_{nb}{}'}{U_{nb}{}'}\right) & w' \end{bmatrix}^{-1} \cdot \begin{bmatrix} Re\left(\frac{H_4(n,1)}{-L\cdot U_{nb}}\right) \\ Im\left(\frac{H_4(n,1)}{-L\cdot U_{nb}}\right) \\ Re\left(\frac{H_4{}'(n,1)}{-L\cdot U_{nb}{}'}\right) \\ Im\left(\frac{H_4{}'(n,1)}{-L\cdot U_{nb}{}'}\right) \end{bmatrix}
\end{aligned}
\tag{17}
$$

where $Re()$ is the real part of a complex number and $Im()$ is the imaginary part of a complex number.

Equations (8) and (11) are the formulas of Algorithm I, which provides an efficient means for rolling-bearing coefficients identification. Equations (16) and (17) are the formulas of Algorithm II, and can be applied to the identification of rolling-bearing coefficients and oil-journal bearing coefficients. The input is m + n + 1 unbalance responses, which can be measured under working conditions. The unbalance responses of the measured bearings must be included.

In engineering, the m + n measuring points can be at the location of the discs and the bearings and the last measuring point can be at any other location on the rotor shaft. There is no need for external excitation and a machine run-down/run-up when using the two algorithms. Moreover, the two proposed methods can be applied to rotors with any discs and any bearings.

2.3. Identification Procedures of the Two Algorithms

The identification procedures of using the proposed algorithms to identify the stiffness and damping coefficients of each disc are defined in Figure 2.

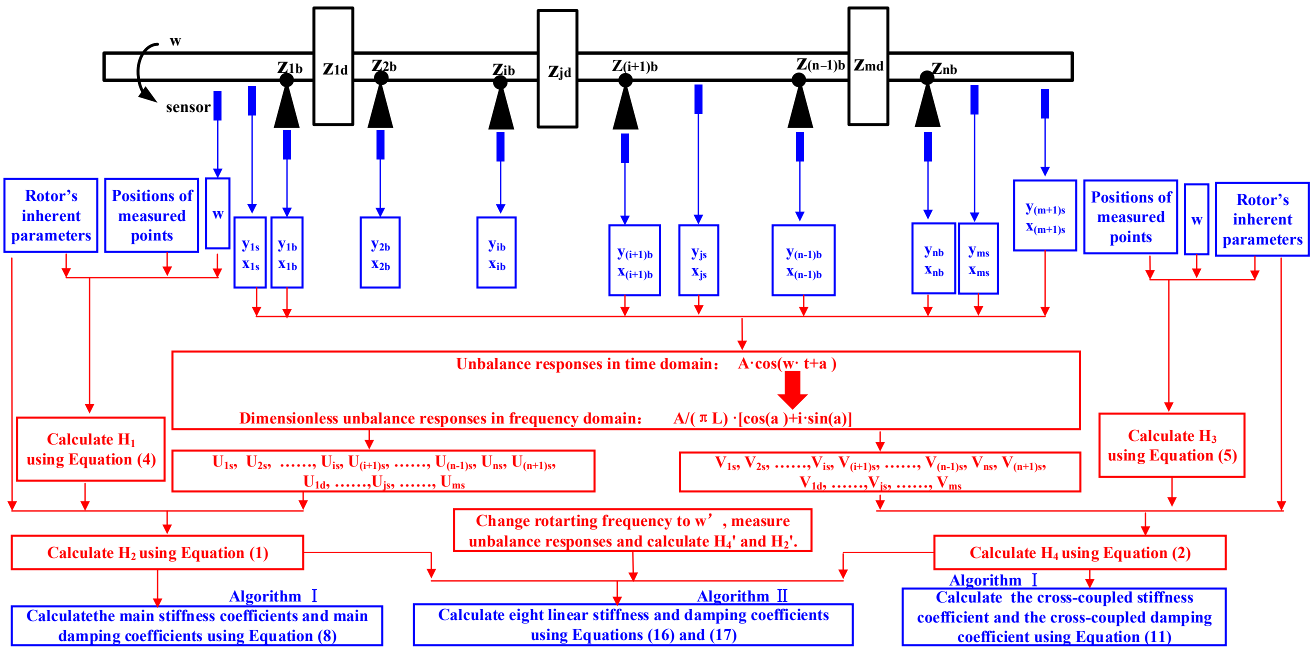

Figure 2. Identification procedures of Algorithm I and Algorithm II.

Step 1: The unbalance responses at each bearing and other m + 1 unbalance responses should be measured and changed to dimensionless unbalance responses in the frequency domain according to Equation (18). Meanwhile, the rotating speed should also be measured. The inherent parameters, which are the length of the shaft, the mass per unit length of the rotor shaft, the elastic modulus of the shaft and the diameter of the shaft, should be known as prior knowledge and the location of the selected measured points on the shaft should also be used as input.

Step 2: The matrices H_1 and H_3 can be calculated according to Equations (4) and (5), respectively. Then, H_2 and H_4 can be calculated according to Equations (1) and (2), respectively.

Step 3: Using H_2 and the dimensionless unbalance responses in the y direction in the frequency domain, each bearing's main stiffness and main damping coefficients in the y direction can be calculated according to Equation (8). According to Equation (11), each bearing's main stiffness and main damping coefficients in the x direction can be obtained using H_4, and the dimensionless unbalance responses in the x direction in the frequency domain. This is the procedure for using Algorithm I.

Step 4: Change the rotating speed slightly to w' and repeat step 1 to step 3 to obtain H_2' and H_4'. Then, using H_2, H_4, H_2' and H_4', the main stiffness coefficients, the main damping coefficients, the cross-coupled stiffness coefficients and the cross-coupled damping coefficients in both x and y directions are calculated according to Equations (16) and (17). These are the identification procedures of using Algorithm II.

$$UD = \frac{A}{\pi L}[\cos(\alpha) + i \cdot \sin(\alpha)] \tag{18}$$

where UD is the dimensionless unbalance responses in the frequency domain; A and α are the amplitude and phase of the unbalance responses in the time domain, respectively.

3. Numerical Simulations and Discussion

3.1. Methodology of Numerical Simulations

Based on Algorithm I and Algorithm II, programs are developed by Matlab for the numerical simulations. In the simulations, the identified bearing coefficients are compared with their setting values for the validation of the two algorithms. Six computational examples are used. They represent single-span and single-disc rotor (g1.1 and h1.1), single-span and four-disc rotor (g1.4 and h1.4), and four-span and four-disc rotor (g4.4 and h4.4). They are supported by rolling bearings and oil-journal bearings. Their parameters are the same as what is listed in Tables 1–6 in reference [26]. The computational example g1.1, g1.4, g4.4, h1.1 and h1.4 are the same as what is shown in Figures 3 and 4 in reference [26]. The computational example h4.4 is shown in Figure 3.

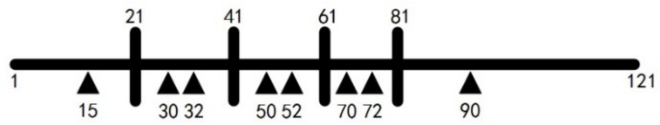

Figure 3. Four-span four-disc rotor supported by oil-journal bearings (h4.4).

Three kinds of numerical simulations are conducted. Firstly, the simulated unbalance responses calculated by CRDAM are fed into Algorithm I and Algorithm II to estimate the bearing coefficients. Secondly, similar identification exercises are performed by contaminating simulated unbalance responses by the set measured error of 5%∠5°. The relative error of the unbalance response amplitude is 5% and the absolute error of the unbalance response angle is 5°. Thirdly, the resolution of the vibration displacement sensor is considered in the simulation. Three kinds of typical sensor resolutions (0.1 nm, 1 nm and 1 um) are considered. By limiting the number of digits after the decimal point in the unbalance responses, the resolution of unbalance responses measurement systems are applied. In the simulations, the calculation rotating frequency is from 1 to 2001 Hz and the interval is 2 Hz.

For simulation validation of Algorithm I, the maximum relative errors of identified main coefficients to the setting values are obtained. For Algorithm II, the maximum relative errors of identified main stiffness and damping coefficients to the setting values and the maximum absolute value of identified cross-coupled stiffness and damping coefficients are obtained in the computational examples g4.4, g1.4 and g1.1. In the computational examples h4.4, h1.4 and h1.1, the maximum relative errors of identified main and cross-coupled coefficients to the setting values are obtained. Moreover, in the third kind of simulation, statistical results of the amount of the frequency point called low error frequency points (LEFPs) are counted. At LEFPs, the relative error of the identified coefficient is less than 10% or the absolute value of the identified coefficient is less than 10.

3.2. Finding of Adjustment Point

3.2.1. Results

The First Kind of Simulation Based on Algorithm I

Using the points in Table 1 as the last measuring points, respectively, eight kinds of simulations are conducted, and then Equations (19)–(22) are obtained using the computational example g4.4. They represent the biggest relative error of the identified main stiffness and damping coefficients of each bearing. The nodes, where the bearings and discs are located, are used as the m + n measuring points in these simulations.

Table 1. The last measuring point.

#14	#29	#33	#49	#53	#69	#73	#91

In Equations (19)–(22), the elements in a row of the matrix are the maximum identification errors of bearing coefficients of #1–#8 bearings, respectively, when using the same point as the last measuring point. For the elements in a column, they are the maximum identification errors of bearing coefficients of the same bearing when the measuring points #14, #29, #33, #49, #53, #69, #73 and #91 are applied, respectively. According to Equations (19)–(22), the results are the following.

(1) #14 point as the last measuring point.

When #14 point, which is near #1 bearing, is used, the maximum identification error of bearing coefficients of #1 disc is the smallest among those of the eight bearings. The maximum identification errors of k1.xx and k1.yy are 5.75×10^{-7}%, and 9.74×10^{-8}%, respectively. They are almost equal to zero. Moreover, the maximum relative errors of c1.xx and c1.yy are also almost equal to zero; although, they are bigger than that of k1.xx and k1.yy. They are only 0.0882% and 0.00795%, respectively.

However, the identification error becomes bigger for some other bearings. For the main stiffness coefficient in the x direction, the biggest of the eight maximum errors, which is 1.19%, occurs at #6 bearing. For the main stiffness coefficient in the y direction, the biggest of the maximum errors occurs at #8 bearing and is 7.94%. While for the main damping coefficients in the x and y directions, they occur at #8 bearing. They are too big and are 389,897% and 924,266%, respectively.

(2) #29 point as the last measuring point.

When #29 point, which is near #2 bearing, is used, the identification error of #2 bearing coefficients is very small; although, it is not the smallest among those of the eight bearings. The maximum relative errors of k2.xx and k2.yy, which are only 5.75×10^{-7}% and 9.74×10^{-8}%, respectively, almost equal zero. Moreover, the maximum relative errors of c2.xx and c2.yy are also almost equal to zero; although, they are bigger than those of k2.xx and k2.yy. They are only 0.0882% and 0.00795%, respectively.

However, the identification error becomes bigger for some other bearings. For the main stiffness coefficient in the x direction, the biggest of the eight maximum errors occurs at #6 bearing. For the main stiffness coefficient in the y direction, the biggest of the maximum errors occurs at #8 bearing. For the main damping coefficients in the x and y directions, they are at #8 bearing. They are too big and are 3878% and 28,609%, respectively.

(3) #33 point as the last measuring point.

When #33 point, which is near #3 bearing, is used, the identification error of #3 bearing coefficients is very small; although, it is not the smallest among those of the eight bearings. The maximum relative errors of k3.xx and k3.yy, which are only 7.88×10^{-6}% and 7.43×10^{-7}%, respectively, almost equal zero. Moreover, the maximum relative errors of c3.xx and c3.yy are also almost equal to zero; although, they are bigger than that of k3.xx and k3.yy. They are only 0.495% and 0.948%, respectively.

However, the identification error becomes bigger for some other bearings. For the main stiffness coefficient in the x direction, the biggest of the eight maximum errors occurs at #6 bearing. For the main stiffness coefficient in the y direction, the biggest of the maximum errors occurs at #8 bearing. For the main damping coefficients in the x and y directions, they are at #8 bearing. They are too big and are 15,859% and 21,915%, respectively.

(4) #49 point as the last measuring point.

When #49 point, which is near #4 bearing, is used, the identification error of #4 bearing coefficients is very small; although, it is not the smallest among the eight bearings. The maximum relative errors of k4.xx and k4.yy, which are only 5.59×10^{-6}% and 6.70×10^{-6}%, respectively, almost equal zero. Moreover, the maximum relative errors of c4.xx and c4.yy are also almost equal to zero; although, they are bigger than that of k4.xx and k4.yy. They are only 0.503% and 0.0455%, respectively.

However, the identification error becomes bigger for some other bearings. For the main stiffness coefficient in the x direction, the biggest of the eight maximum errors occurs at #7 bearing. For the main stiffness coefficient in the y direction, the biggest of the maximum errors is at #8 bearing. For the main damping coefficients in the x and y directions, they are at #8 bearing and are 702% and 456%, respectively.

(5) #53 point as the last measuring point.

When #53 point, which is near #5 bearing, is used, the identification error of #5 bearing coefficients is the smallest among the eight bearings. The maximum relative errors of k5.xx and k5.yy, which are only 5.03×10^{-5}% and 2.16×10^{-5}%, respectively, almost equal zero. Moreover, the maximum relative errors of c5.xx and c5.yy are also almost equal to zero; although, they are bigger than that of k5.xx and k5.yy. They are only 1.60% and 3.52%, respectively.

However, the identification error becomes bigger for some other bearings. For the main stiffness coefficient in the x direction, the biggest of the eight maximum errors occurs at #6 bearing. For the main stiffness coefficient in the y direction, the biggest of the maximum errors occurs at #2 bearing. For the main damping coefficients in the x and y directions, they are at #1 bearing and are 512% and 420%, respectively.

(6) #69 point as the last measuring point.

When #69 point, which is near #6 bearing, is used, the identification error of #6 bearing coefficients is very small; although, it is not the smallest among the eight bearings. The maximum relative errors of k6.xx and k6.yy, which are only 8.03×10^{-6}% and 8.19×10^{-6}%, respectively, almost equal zero. Moreover, the maximum relative errors of c6.xx and c6.yy are also almost equal to zero; although, they are bigger than that of k6.xx and k6.yy. They are only 0.332% and 0.540%, respectively.

However, the identification error becomes bigger for some other bearings. For the main stiffness and damping coefficients in the x and y directions, the biggest values of the eight maximum errors occur at #1 bearing. For the main damping coefficients in the x and y directions, they are at #1 bearing and are 5169% and 2235%, respectively.

(7) #73 point as the last measuring point.

When #73 point, which is near #7 bearing, is used, the identification error of #7 bearing coefficients is very small; although, it is not the smallest among the eight bearings. The maximum relative errors of k7.xx and k7.yy, which are only 5.28×10^{-6}% and 7.84×10^{-6}%, respectively, almost equal zero. Moreover, the maximum relative errors of c7.xx and c7.yy are also almost equal to zero; although, they are bigger than those of k7.xx and k7.yy. They are only 0.223% and 0.0215%, respectively.

However, the identification error becomes bigger for some other bearings. For the main stiffness and damping coefficients in the x and y directions, the biggest values of the eight maximum errors occur at #1 bearing. For the main damping coefficients in the x and y directions, they are at #1 bearing and are 14,705% and 42,741%, respectively.

(8) #91 point as the last measuring point.

When #91 point, which is near #8 bearing, is used, the identification error of #8 bearing coefficients is the smallest among the eight bearings. The maximum relative errors of k8.xx and k8.yy, which are only 1.91×10^{-7}% and 5.98×10^{-8}%, respectively, almost equal zero. Moreover, the maximum relative errors of c8.xx and c8.yy are also almost equal to zero; although, they are bigger than that of k8.xx and k8.yy. They are only 0.00755% and 0.000922%, respectively.

However, the identification error becomes bigger for some other bearings. For the main stiffness coefficient in the x direction, the biggest of the eight maximum errors occurs at #3 bearing. For the main stiffness coefficient in the y direction, the biggest of the maximum errors occurs at #3 bearing. For the main damping coefficient in the x direction, the biggest of the maximum errors is much bigger. It occurs at #2 bearing and is 11,985%. For the main damping coefficient in the y direction, the biggest of the eight maximum errors, which is 10,846%, occurs at #1 bearing.

$$A1-Kxx_{g44} = \begin{array}{c} \\ \#14P \\ \#29P \\ \#33P \\ \#49P \\ \#53P \\ \#69P \\ \#73P \\ \#91P \end{array} \begin{array}{c} \begin{array}{cccccccc} \#1B & \#2B & \#3B & \#4B & \#5B & \#6B & \#7B & \#8B \end{array} \\ \left[\begin{array}{cccccccc} 5.75\times10^{-7} & 3.85\times10^{-5} & 3.34\times10^{-5} & 0.0127 & 0.0575 & 1.19 & 0.434 & 0.695 \\ 4.36\times10^{-6} & 2.84\times10^{-6} & 4.16\times10^{-6} & 0.00246 & 0.0111 & 0.235 & 0.0887 & 0.204 \\ 3.57\times10^{-5} & 2.00\times10^{-5} & 7.88\times10^{-6} & 0.000774 & 0.00387 & 0.119 & 0.0735 & 0.0417 \\ 0.000168 & 3.33\times10^{-5} & 0.000106 & 5.59\times10^{-6} & 6.82\times10^{-5} & 0.000459 & 0.000974 & 0.00518 \\ 0.00115 & 0.000970 & 0.000390 & 5.76\times10^{-5} & 5.03\times10^{-5} & 0.000666 & 0.000266 & 0.000255 \\ 0.0229 & 0.0148 & 0.0194 & 2.10\times10^{-5} & 0.000212 & 8.03\times10^{-6} & 1.82\times10^{-5} & 2.79\times10^{-5} \\ 0.154 & 0.0769 & 0.0934 & 0.000940 & 0.00237 & 2.98\times10^{-5} & 5.28\times10^{-6} & 6.00\times10^{-6} \\ 0.0519 & 0.147 & 0.211 & 0.000302 & 0.00182 & 0.0001159 & 4.73\times10^{-5} & 1.91\times10^{-7} \end{array} \right] \end{array} \quad (19)$$

$$A1-Kyy_{g44} = \begin{array}{c} \\ \#14P \\ \#29P \\ \#33P \\ \#49P \\ \#53P \\ \#69P \\ \#73P \\ \#91P \end{array} \begin{array}{c} \begin{array}{cccccccc} \#1B & \#2B & \#3B & \#4B & \#5B & \#6B & \#7B & \#8B \end{array} \\ \left[\begin{array}{cccccccc} 9.74\times10^{-8} & 0.000137 & 0.000322 & 0.0272 & 0.142 & 5.32 & 3.76 & 7.92 \\ 4.13\times10^{-6} & 7.08\times10^{-6} & 2.68\times10^{-5} & 0.000259 & 0.00210 & 0.145 & 0.133 & 0.597 \\ 6.16\times10^{-5} & 2.53\times10^{-5} & 7.43\times10^{-7} & 0.000722 & 0.00379 & 0.139 & 0.0991 & 0.150 \\ 6.83\times10^{-5} & 0.000437 & 0.000490 & 6.70\times10^{-6} & 7.61\times10^{-5} & 0.00646 & 0.00534 & 0.00650 \\ 0.000546 & 0.000922 & 0.000321 & 2.28\times10^{-5} & 2.16\times10^{-5} & 0.000498 & 0.000216 & 0.000192 \\ 0.00358 & 0.00149 & 0.00175 & 0.000144 & 0.000230 & 8.19\times10^{-6} & 4.84\times10^{-6} & 1.43\times10^{-5} \\ 0.0999 & 0.0182 & 0.814 & 0.00132 & 0.00125 & 3.46\times10^{-5} & 7.84\times10^{-6} & 1.26\times10^{-5} \\ 0.0185 & 0.0532 & 0.115 & 0.00104 & 0.000430 & 4.79\times10^{-5} & 1.83\times10^{-5} & 5.98\times10^{-8} \end{array} \right] \end{array} \quad (20)$$

$$A1-Cxx_{g44} = \begin{array}{c} \\ \#14P \\ \#29P \\ \#33P \\ \#49P \\ \#53P \\ \#69P \\ \#73P \\ \#91P \end{array} \begin{array}{c} \begin{array}{cccccccc} \#1B & \#2B & \#3B & \#4B & \#5B & \#6B & \#7B & \#8B \end{array} \\ \left[\begin{array}{cccccccc} 0.0882 & 5.72 & 22.2 & 95.6 & 1083 & 179713 & 187922 & 389897 \\ 0.669 & 0.436 & 1.644 & 22.7 & 191 & 34293 & 36147 & 73878 \\ 4.25 & 0.695 & 0.495 & 45.5 & 111 & 7595 & 10478 & 15859 \\ 105 & 24.7 & 27.2 & 0.503 & 7.60 & 402 & 333 & 702 \\ 512 & 146 & 220 & 0.607 & 1.60 & 91.7 & 98.3 & 191 \\ 5169 & 972 & 29.3 & 54.5 & 89.8 & 0.332 & 0.354 & 3.59 \\ 14705 & 2328 & 3093 & 281 & 375 & 0.0995 & 0.223 & 0.0620 \\ 5045 & 11985 & 2611 & 639 & 1113 & 9.72 & 1.39 & 0.00755 \end{array} \right] \end{array} \quad (21)$$

$$A1-Cyy_{g44} = \begin{array}{c} \\ \#14P \\ \#29P \\ \#33P \\ \#49P \\ \#53P \\ \#69P \\ \#73P \\ \#91P \end{array} \begin{array}{c} \begin{array}{cccccccc} \#1B & \#2B & \#3B & \#4B & \#5B & \#6B & \#7B & \#8B \end{array} \\ \left[\begin{array}{cccccccc} 0.00795 & 5.25 & 40.9 & 2761 & 8824 & 190712 & 358496 & 924266 \\ 0.150 & 0.161 & 0.888 & 115 & 472 & 5714 & 993 & 28609 \\ 0.366 & 1.19 & 0.948 & 74.8 & 238 & 4857 & 9290 & 21915 \\ 38.7 & 3.36 & 27.5 & 0.0455 & 13.1 & 43.8 & 215 & 456 \\ 420 & 91.7 & 163 & 1.07 & 3.52 & 65.8 & 71.3 & 158 \\ 2235 & 462 & 570 & 3.79 & 15.5 & 0.534 & 0.274 & 1.99 \\ 42741 & 7580 & 6283 & 298 & 513 & 5.05 & 0.0215 & 1.01 \\ 10846 & 8473 & 5519 & 392 & 674 & 5.86 & 0.916 & 0.000922 \end{array} \right] \end{array} \quad (22)$$

where $A1-Kxx_{g44}$, $A1-Kyy_{g44}$, $A1-Cxx_{g44}$ and $A1-Cyy_{g44}$ are the matrices of the maximum identification error of the main stiffness coefficient in the x direction, the main stiffness coefficient in the y direction, the main damping coefficient in the x direction and the main damping coefficient in the y direction of #1 to #8 bearings under different last measuring point conditions in the simulation of g4.4 using Algorithm I; the red numbers show the best identification results when the last measuring point is changed.

The First Kind of Simulation Based on Algorithm II

(1) Results of the computational example g4.4.

Equations (23)–(30) can be obtained using the computational example g4.4 when the points #14, #29, #33, #49, #53, #69, #73 and #91 points are used as the last measuring point, respectively. It shows the maximum relative errors of each bearing's main coefficients and the maximum absolute value of each bearing's cross-coupled coefficients. The nodes, where the bearings and discs are located, are used as the m + n measuring points.

According to the first rows of the matrix in Equations (23)–(30), the identification error of #1 bearing coefficients is the smallest among the eight bearings when #14 point is used. For the identified main coefficients, the maximum relative errors of k1.xx and k1.yy, which are only 6.89×10^{-7}% and 2.13×10^{-7}%, respectively, almost equal zero. Moreover, the maximum relative errors of c1.xx and c1.yy are also almost equal to zero; although, they are bigger than that of k1.xx and k1.yy. They are only 0.0179% and 0.0945%, respectively. While for the cross-coupled coefficients, the identification errors of cross-coupled damping coefficients are bigger than those of cross-coupled stiffness coefficients; although, they are almost equal to zero (the setting value). The maximum absolute values of k1.xy and k1.yx are 0.0945 and 0.135, respectively. The maximum absolute values of c1.xy and c1.yx are 0.0210 and 0.00298, respectively.

However, the identification error becomes bigger for some other bearings. For the main stiffness coefficient in the x direction, the biggest of the eight maximum errors, which is 2.67%, occurs at #8 bearing. For the main stiffness coefficient in the y direction, the biggest of the maximum errors occurs at #8 bearing and is 9.53%. While for the four main damping coefficients in the x and y directions, the biggest values of the maximum errors are much bigger. They occur at #8 bearing and are 76,824% and 183,620%, respectively. For the cross-coupled coefficients, the biggest values of the maximum errors, which are 369,059, 325,011, 12,758 and 143,445, occur at #8, #7, #8 and #8 bearing, respectively.

By changing the last measuring point to #29, #33, #49, #53, #69, #73 and #91 points, respectively, similar results can be obtained according to the other rows of the matrices in Equations (23)–(30).

$$A2-Kxx_{g44} = \begin{array}{cc} & \begin{matrix} \#1B & \#2B & \#3B & \#4B & \#5B & \#6B & \#7B & \#8B \end{matrix} \\ \begin{matrix} \#14P \\ \#29P \\ \#33P \\ \#49P \\ \#53P \\ \#69P \\ \#73P \\ \#91P \end{matrix} & \begin{bmatrix} 6.89\times10^{-7} & 4.59\times10^{-5} & 4.04\times10^{-5} & 0.0152 & 0.0687 & 1.41 & 0.514 & 2.67 \\ 6.37\times10^{-6} & 3.41\times10^{-6} & 1.21\times10^{-5} & 0.00295 & 0.0134 & 0.284 & 0.220 & 0.327 \\ 0.000102 & 2.41\times10^{-5} & 9.38\times10^{-6} & 0.000930 & 0.00524 & 0.143 & 0.0887 & 0.208 \\ 0.000201 & 6.44\times10^{-5} & 0.000125 & 6.71\times10^{-6} & 8.20\times10^{-5} & 0.000788 & 0.00142 & 0.00618 \\ 0.00137 & 0.00116 & 0.000479 & 6.90\times10^{-5} & 6.04\times10^{-5} & 0.000797 & 0.000321 & 0.000429 \\ 0.0274 & 0.0178 & 0.0232 & 6.17\times10^{-5} & 0.000372 & 9.65\times10^{-6} & 2.18\times10^{-5} & 7.78\times10^{-5} \\ 0.185 & 0.0924 & 0.112 & 0.00112 & 0.00282 & 3.58\times10^{-5} & 6.33\times10^{-6} & 7.23\times10^{-6} \\ 0.213 & 0.270 & 0.253 & 0.0105 & 0.0166 & 0.000262 & 8.30\times10^{-5} & 2.38\times10^{-7} \end{bmatrix} \end{array} \tag{23}$$

$$A2-Cxx_{g44} = \begin{array}{cc} & \begin{matrix} \#1B & \#2B & \#3B & \#4B & \#5B & \#6B & \#7B & \#8B \end{matrix} \\ \begin{matrix} \#14P \\ \#29P \\ \#33P \\ \#49P \\ \#53P \\ \#69P \\ \#73P \\ \#91P \end{matrix} & \begin{bmatrix} 0.0179 & 1.13 & 4.32 & 18.2 & 229 & 35442 & 36599 & 76824 \\ 0.128 & 0.0869 & 0.330 & 7.33 & 25.4 & 6703 & 7211 & 14857 \\ 0.850 & 0.144 & 0.0963 & 9.46 & 23.8 & 1538 & 2123 & 3265 \\ 20.7 & 4.84 & 5.36 & 0.0967 & 1.47 & 78.8 & 65.4 & 138 \\ 101 & 29.1 & 43.9 & 0.132 & 0.309 & 18.3 & 19.6 & 38.1 \\ 1012 & 189 & 16.4 & 10.8 & 17.8 & 0.0734 & 0.0621 & 0.698 \\ 3017 & 491 & 587 & 57.1 & 76.7 & 0.0202 & 0.0437 & 0.00965 \\ 911 & 2428 & 555 & 130 & 226 & 1.96 & 0.285 & 0.00145 \end{bmatrix} \end{array} \tag{24}$$

$$A2-Kyy_{g44} = \begin{array}{cc} & \begin{matrix} \#1B & \#2B & \#3B & \#4B & \#5B & \#6B & \#7B & \#8B \end{matrix} \\ \begin{matrix} \#14P \\ \#29P \\ \#33P \\ \#49P \\ \#53P \\ \#69P \\ \#73P \\ \#91P \end{matrix} & \begin{bmatrix} 2.13\times10^{-7} & 0.000165 & 0.000385 & 0.0327 & 0.173 & 6.39 & 4.52 & 9.53 \\ 7.74\times10^{-6} & 8.49\times10^{-6} & 3.21\times10^{-5} & 0.000950 & 0.00632 & 0.316 & 0.407 & 0.715 \\ 0.000125 & 3.02\times10^{-5} & 1.28\times10^{-6} & 0.000871 & 0.00456 & 0.183 & 0.208 & 0.365 \\ 0.000123 & 0.000525 & 0.000586 & 8.03\times10^{-6} & 9.19\times10^{-5} & 0.00776 & 0.00641 & 0.00781 \\ 0.000671 & 0.00111 & 0.000388 & 2.74\times10^{-5} & 2.59\times10^{-5} & 0.000605 & 0.000263 & 0.000283 \\ 0.0160 & 0.00236 & 0.00293 & 0.000173 & 0.000275 & 9.80\times10^{-6} & 5.84\times10^{-6} & 1.73\times10^{-5} \\ 0.120 & 0.0218 & 0.0980 & 0.00157 & 0.00207 & 4.13\times10^{-5} & 9.38\times10^{-6} & 1.51\times10^{-5} \\ 0.0837 & 0.236 & 0.280 & 0.0101 & 0.0164 & 0.000192 & 6.97\times10^{-5} & 1.61\times10^{-7} \end{bmatrix} \end{array} \tag{25}$$

$$A2-Cyy_{g44}=\begin{array}{cc} & \begin{array}{cccccccc} \#1B & \#2B & \#3B & \#4B & \#5B & \#6B & \#7B & \#8B \end{array} \\ \begin{array}{c} \#14P \\ \#29P \\ \#33P \\ \#49P \\ \#53P \\ \#69P \\ \#73P \\ \#91P \end{array} & \begin{bmatrix} 0.00130 & 1.02 & 8.16 & 554 & 1764 & 37038 & 71313 & 183620 \\ 0.0345 & 0.0273 & 0.181 & 23.4 & 96.5 & 1267 & 186 & 5303 \\ 0.185 & 0.252 & 0.187 & 14.3 & 43.8 & 1061 & 1923 & 4489 \\ 8.02 & 0.742 & 5.50 & 0.0211 & 2.63 & 10.3 & 42.3 & 90.5 \\ 80.5 & 17.7 & 32.6 & 0.181 & 0.680 & 12.7 & 14.1 & 31.5 \\ 468 & 96.9 & 116 & 0.949 & 3.46 & 0.107 & 0.0594 & 0.409 \\ 8540 & 1504 & 1228 & 59.7 & 103 & 1.00 & 0.00685 & 0.199 \\ 1852 & 1595 & 1018 & 75.2 & 129 & 1.10 & 0.165 & 0.000174 \end{bmatrix} \end{array} \quad (26)$$

$$A2-Kxy_{g44}=\begin{array}{cc} & \begin{array}{cccccccc} \#1B & \#2B & \#3B & \#4B & \#5B & \#6B & \#7B & \#8B \end{array} \\ \begin{array}{c} \#14P \\ \#29P \\ \#33P \\ \#49P \\ \#53P \\ \#69P \\ \#73P \\ \#91P \end{array} & \begin{bmatrix} 0.0945 & 5.44 & 20.9 & 188 & 1207 & 169914 & 178123 & 369059 \\ 1.84 & 0.416 & 1.56 & 188 & 1158 & 40398 & 34398 & 70167 \\ 18.8 & 1.47 & 0.465 & 48.7 & 577 & 13264 & 11645 & 21011 \\ 96.5 & 23.4 & 25.7 & 0.477 & 7.14 & 380 & 316 & 664 \\ 467 & 140 & 208 & 0.632 & 1.51 & 86.9 & 93.5 & 181 \\ 5232 & 923 & 438 & 52.0 & 84.6 & 0.320 & 0.659 & 3.39 \\ 14927 & 2242 & 2909 & 269 & 355 & 1.09 & 0.213 & 0.824 \\ 20565 & 11457 & 41342 & 611 & 1145 & 9.24 & 4.86 & 0.0108 \end{bmatrix} \end{array} \quad (27)$$

$$A2-Kyx_{g44}=\begin{array}{cc} & \begin{array}{cccccccc} \#1B & \#2B & \#3B & \#4B & \#5B & \#6B & \#7B & \#8B \end{array} \\ \begin{array}{c} \#14P \\ \#29P \\ \#33P \\ \#49P \\ \#53P \\ \#69P \\ \#73P \\ \#91P \end{array} & \begin{bmatrix} 0.135 & 4.74 & 37.3 & 2502 & 8090 & 173327 & 325011 & 219685 \\ 2.07 & 0.566 & 1.03 & 230 & 1059 & 51095 & 29962 & 17229 \\ 26.7 & 2.08 & 0.864 & 106 & 498 & 21106 & 9260 & 15441 \\ 32.0 & 3.81 & 25.1 & 0.408 & 12.0 & 59.8 & 194 & 149 \\ 343 & 82.6 & 149 & 0.945 & 3.20 & 59.7 & 64.6 & 39.8 \\ 2620 & 422 & 522 & 7.72 & 15.0 & 0.492 & 0.551 & 1.73 \\ 35142 & 6858 & 5721 & 270 & 470 & 4.59 & 0.162 & 0.921 \\ 15428 & 39749 & 28480 & 575 & 624 & 12.9 & 6.43 & 0.0137 \end{bmatrix} \end{array} \quad (28)$$

$$A2-Cxy_{g44}=\begin{array}{cc} & \begin{array}{cccccccc} \#1B & \#2B & \#3B & \#4B & \#5B & \#6B & \#7B & \#8B \end{array} \\ \begin{array}{c} \#14P \\ \#29P \\ \#33P \\ \#49P \\ \#53P \\ \#69P \\ \#73P \\ \#91P \end{array} & \begin{bmatrix} 0.0210 & 0.661 & 0.527 & 221 & 983 & 20020 & 6934 & 12758 \\ 0.170 & 0.0520 & 0.0807 & 44.3 & 201 & 4484 & 1874 & 2968 \\ 1.38 & 0.364 & 0.135 & 14.1 & 69.8 & 2172 & 1352 & 819 \\ 6.17 & 0.603 & 1.83 & 0.0987 & 1.19 & 8.11 & 16.6 & 89.8 \\ 42.0 & 17.5 & 7.11 & 1.03 & 0.888 & 11.9 & 4.84 & 5.17 \\ 821 & 264 & 341 & 0.411 & 3.90 & 0.143 & 0.322 & 0.496 \\ 5675 & 1386 & 1677 & 16.4 & 41.4 & 0.535 & 0.0941 & 0.110 \\ 1736 & 2663 & 3798 & 5.56 & 32.6 & 2.09 & 0.854 & 0.00331 \end{bmatrix} \end{array} \quad (29)$$

$$A2-Cyx_{g44}=\begin{array}{cc} & \begin{array}{cccccccc} \#1B & \#2B & \#3B & \#4B & \#5B & \#6B & \#7B & \#8B \end{array} \\ \begin{array}{c} \#14P \\ \#29P \\ \#33P \\ \#49P \\ \#53P \\ \#69P \\ \#73P \\ \#91P \end{array} & \begin{bmatrix} 0.00298 & 2.46 & 5.85 & 485 & 2591 & 95895 & 67788 & 143445 \\ 0.150 & 0.126 & 0.480 & 4.19 & 36.4 & 2619 & 2413 & 10651 \\ 2.21 & 0.443 & 0.0164 & 13.2 & 69.2 & 2467 & 1717 & 2522 \\ 2.20 & 7.83 & 8.86 & 0.120 & 1.37 & 117 & 96.2 & 118 \\ 22.5 & 17.2 & 6.77 & 0.410 & 0.381 & 9.40 & 4.31 & 4.52 \\ 141 & 23.3 & 36.1 & 2.62 & 4.16 & 0.143 & 0.0894 & 0.268 \\ 3552 & 333 & 1472 & 23.1 & 22.0 & 0.623 & 0.138 & 0.228 \\ 572 & 912 & 1981 & 17.3 & 6.462 & 0.831 & 0.3101 & 0.000972 \end{bmatrix} \end{array} \quad (30)$$

where $A2-Kxx_{g44}$, $A2-Kyy_{g44}$, $A2-Cxx_{g44}$, $A2-Cyy_{g44}$,$A2-Kxy_{g44}$, $A2-Kyx_{g44}$, $A2-Cxy_{g44}$ and $A2-Cyx_{g44}$ are the matrices of the maximum identification error of the main stiffness coefficient in the x direction, the main stiffness coefficient in the y direction, the main damping coefficient in the x direction, the main damping coefficient in the y direction, the cross-coupled stiffness coefficient in the x direction, the cross-coupled stiffness coefficient in the y direction, the cross-coupled damping coefficient in the x direction and the cross-coupled damping coefficient in the y direction of #1 to #8 bearings under different last measuring point condition in the simulation of g4.4 using Algorithm II; the red numbers show the best identification results when the last measuring point is changed.

(2) Results of the Computational Example h4.4.

For rotor h4.4 supported by oil journal bearings, Equations (31)–(38), which show the biggest relative errors of each bearing's main and cross-coupled coefficients, are obtained using #14, #29, #31, #49, #51, #69, #71 and #89 point as the last one measuring point, respectively. The nodes, where the bearings and discs are located, are used as the m + n measuring points.

According to the first rows of the matrices in Equations (31)–(38), the identification error of #1 bearing coefficients is very small; although, it is not the smallest among the eight bearings. For the stiffness coefficients, the maximum relative error of k1.xx, k1.yy, k1.xy and k1.yx are 0.444%, 0.346%, 1.23% and 0.514%, respectively. While for the damping coefficients, the maximum relative error of c1.xx, c1.yy, c1.xy and c1.yx, which are 0.00337%, 0.00490%, 0.0634% and 0.0209%, respectively, are smaller than that of the stiffness coefficients.

However, the identification error becomes bigger for some other bearings. For the main stiffness coefficient in the x direction, the biggest of the eight maximum errors, which is 102%, occurs at #7 bearing. For the main stiffness coefficient in the y direction, the biggest of the maximum errors occurs at #7 bearing and is 1054%. While for the four main damping coefficients in the x and y directions, the biggest values of the maximum errors are much smaller. They occur at #7 bearing and are 2.59% and 9.51%, respectively. For the cross-coupled coefficients, they are 61.0%, 499%, 3.22% and 23.4%, respectively, and they occur at #7, #7, #8 and #7 bearings, respectively.

By changing the last measuring point to other points listed in Table 2, respectively, similar results can be obtained according to the other rows of the matrices in Equations (31)–(38).

$$A2-Kxx_{h44}=\begin{array}{cc}
 & \begin{array}{cccccccc} \#1B & \#2B & \#3B & \#4B & \#5B & \#6B & \#7B & \#8B \end{array} \\
\begin{array}{c} \#14P \\ \#29P \\ \#31P \\ \#49P \\ \#51P \\ \#69P \\ \#71P \\ \#89P \end{array} & \left[\begin{array}{cccccccc}
0.444 & 0.0489 & 1.976 & 3.83 & 9.18 & 2.70 & 102 & 8.52 \\
0.482 & 0.0148 & 0.682 & 0.230 & 0.750 & 12.4 & 94.0 & 586 \\
1.79 & 0.0424 & 0.673 & 0.324 & 1.05 & 17.4 & 132 & 854 \\
4.27 & 0.00675 & 0.743 & 0.000898 & 0.000540 & 0.0113 & 0.205 & 5.24 \\
69.4 & 0.0629 & 0.658 & 0.000775 & 0.00119 & 0.00499 & 0.0620 & 0.541 \\
134 & 1.22 & 18.9 & 0.00660 & 0.00959 & 0.000199 & 0.00622 & 0.161 \\
944 & 7.18 & 35.8 & 0.0187 & 0.00690 & 0.000207 & 0.00635 & 0.0280 \\
53.4 & 25.5 & 44.7 & 0.0514 & 0.155 & 0.00144 & 0.0140 & 0.0591
\end{array}\right]
\end{array} \tag{31}$$

$$A2-Cxx_{h44}=\begin{array}{cc}
 & \begin{array}{cccccccc} \#1B & \#2B & \#3B & \#4B & \#5B & \#6B & \#7B & \#8B \end{array} \\
\begin{array}{c} \#14P \\ \#29P \\ \#31P \\ \#49P \\ \#51P \\ \#69P \\ \#71P \\ \#89P \end{array} & \left[\begin{array}{cccccccc}
0.00337 & 0.0111 & 0.0938 & 0.149 & 0.0551 & 0.629 & 2.594 & 0.262 \\
0.00366 & 0.000564 & 0.0268 & 0.0159 & 0.00248 & 0.106 & 0.362 & 8.18 \\
0.0203 & 0.00167 & 0.0264 & 0.0227 & 0.00341 & 0.439 & 2.02 & 12.0 \\
0.0325 & 0.000606 & 0.0296 & 4.98\times10^{-5} & 2.39\times10^{-5} & 0.00190 & 0.00671 & 0.00887 \\
0.530 & 0.00183 & 0.0272 & 4.04\times10^{-5} & 2.40\times10^{-5} & 0.000947 & 0.001978 & 0.0232 \\
2.38 & 0.103 & 0.859 & 0.000397 & 6.51\times10^{-5} & 1.26\times10^{-5} & 0.000200 & 0.00101 \\
7.14 & 0.307 & 1.38 & 0.000479 & 0.000666 & 2.13\times10^{-5} & 0.000214 & 0.000408 \\
0.4038 & 0.547 & 2.00 & 0.0170 & 0.00527 & 0.000332 & 0.000408 & 0.000497
\end{array}\right]
\end{array} \tag{32}$$

$$A2-Kyy_{h44}=\begin{array}{cc}
 & \begin{array}{cccccccc} \#1B & \#2B & \#3B & \#4B & \#5B & \#6B & \#7B & \#8B \end{array} \\
\begin{array}{c} \#14P \\ \#29P \\ \#31P \\ \#49P \\ \#51P \\ \#69P \\ \#71P \\ \#89P \end{array} & \left[\begin{array}{cccccccc}
0.346 & 0.159 & 2.95 & 10.4 & 14.7 & 12.5 & 1054 & 178 \\
0.634 & 0.0199 & 1.60 & 1.77 & 2.20 & 19.4 & 564 & 7679 \\
2.68 & 0.0596 & 1.63 & 2.53 & 2.96 & 27.4 & 879 & 8720 \\
3.46 & 0.0384 & 1.85 & 0.00436 & 0.00337 & 0.0508 & 2.01 & 75.7 \\
24.1 & 0.726 & 3.70 & 0.00201 & 0.00494 & 0.00826 & 0.406 & 125 \\
176 & 11.4 & 46.7 & 0.142 & 0.0781 & 0.000415 & 0.0190 & 0.398 \\
592 & 7.51 & 61.6 & 0.256 & 0.0892 & 0.000842 & 0.00913 & 1.07 \\
8.57 & 166 & 175 & 2.15 & 0.749 & 0.00815 & 0.0986 & 0.628
\end{array}\right]
\end{array} \tag{33}$$

$$A2 - Cyy_{h44} = \begin{bmatrix} & \#1B & \#2B & \#3B & \#4B & \#5B & \#6B & \#7B & \#8B \\ \#14P & 0.00490 & 0.00295 & 0.0610 & 0.00972 & 0.00753 & 0.758 & 9.51 & 0.193 \\ \#29P & 0.0150 & 0.000540 & 0.0282 & 0.00607 & 0.00351 & 0.963 & 5.13 & 8.04 \\ \#31P & 0.0946 & 0.00147 & 0.0288 & 0.00749 & 0.00707 & 1.44 & 7.90 & 10.9 \\ \#49P & 0.0430 & 0.000613 & 0.0329 & 1.91 \times 10^{-5} & 1.59 \times 10^{-5} & 0.00292 & 0.0180 & 0.0102 \\ \#51P & 0.438 & 0.00449 & 0.0652 & 2.98 \times 10^{-5} & 1.34 \times 10^{-5} & 0.000332 & 0.00341 & 0.0482 \\ \#69P & 1.65 & 0.197 & 1.12 & 0.000498 & 0.000102 & 2.90 \times 10^{-5} & 0.000173 & 0.000844 \\ \#71P & 29.3 & 0.419 & 0.467 & 0.000441 & 0.000468 & 4.81 \times 10^{-5} & 7.92 \times 10^{-5} & 0.000118 \\ \#89P & 0.206 & 0.845 & 1.63 & 0.00443 & 0.00544 & 0.000410 & 0.000892 & 5.57 \times 10^{-5} \end{bmatrix} \quad (34)$$

$$A2 - Kxy_{h44} = \begin{bmatrix} & \#1B & \#2B & \#3B & \#4B & \#5B & \#6B & \#7B & \#8B \\ \#14P & 1.23 & 0.303 & 0.789 & 45.0 & 45.6 & 29.7 & 61.0 & 28.5 \\ \#29P & 1.97 & 0.0931 & 0.285 & 3.12 & 3.77 & 48.7 & 26.4 & 1598 \\ \#31P & 6.71 & 0.266 & 0.282 & 4.42 & 5.28 & 68.2 & 45.1 & 2337 \\ \#49P & 6.09 & 0.0418 & 0.310 & 0.0114 & 0.00255 & 0.103 & 0.144 & 0.807 \\ \#51P & 81.1 & 0.397 & 0.272 & 0.00972 & 0.00580 & 0.0608 & 0.0429 & 3.83 \\ \#69P & 1240 & 7.61 & 7.66 & 0.0859 & 0.0485 & 0.000627 & 0.00432 & 0.123 \\ \#71P & 1179 & 45.3 & 15.1 & 0.1487 & 0.0316 & 0.00202 & 0.00455 & 0.0794 \\ \#89P & 57.3 & 158 & 18.1 & 1.29 & 0.819 & 0.0203 & 0.00913 & 0.0668 \end{bmatrix} \quad (35)$$

$$A2 - Kyx_{h44} = \begin{bmatrix} & \#1B & \#2B & \#3B & \#4B & \#5B & \#6B & \#7B & \#8B \\ \#14P & 0.514 & 0.0849 & 2.867 & 3.36 & 7.83 & 14.6 & 499 & 22.0 \\ \#29P & 1.57 & 0.0107 & 1.50 & 0.515 & 1.18 & 27.5 & 263 & 2744 \\ \#31P & 9.91 & 0.0319 & 1.53 & 0.752 & 1.59 & 36.4 & 419 & 3885 \\ \#49P & 4.49 & 0.0208 & 1.74 & 0.00121 & 0.00184 & 0.0446 & 0.970 & 4.05 \\ \#51P & 45.8 & 0.384 & 3.48 & 0.000416 & 0.00267 & 0.0171 & 0.214 & 8.82 \\ \#69P & 175 & 6.08 & 47.0 & 0.0410 & 0.0418 & 0.000668 & 0.00885 & 0.328 \\ \#71P & 3068 & 4.01 & 52.2 & 0.0804 & 0.0487 & 0.00189 & 0.00457 & 0.155 \\ \#89P & 20.9 & 88.3 & 149 & 0.679 & 0.415 & 0.00370 & 0.0465 & 0.0852 \end{bmatrix} \quad (36)$$

$$A2 - Cxy_{h44} = \begin{bmatrix} & \#1B & \#2B & \#3B & \#4B & \#5B & \#6B & \#7B & \#8B \\ \#14P & 0.0634 & 0.0100 & 0.117 & 0.0844 & 0.0661 & 1.51 & 3.16 & 3.22 \\ \#29P & 0.0688 & 0.000508 & 0.0339 & 0.0116 & 0.00178 & 0.219 & 0.445 & 11.7 \\ \#31P & 0.322 & 0.00150 & 0.0334 & 0.0167 & 0.00218 & 1.10 & 2.49 & 16.9 \\ \#49P & 0.610 & 0.000808 & 0.0373 & 3.39 \times 10^{-5} & 4.29 \times 10^{-5} & 0.00543 & 0.00835 & 0.319 \\ \#51P & 9.93 & 0.00192 & 0.0342 & 2.68 \times 10^{-5} & 3.71 \times 10^{-5} & 0.00225 & 0.00246 & 0.0914 \\ \#69P & 28.6 & 0.0922 & 1.08 & 0.000278 & 0.000160 & 3.26 \times 10^{-5} & 0.000249 & 0.0117 \\ \#71P & 135 & 0.276 & 1.74 & 0.000729 & 0.000670 & 2.57 \times 10^{-5} & 0.000267 & 0.000512 \\ \#89P & 7.61 & 0.514 & 2.51 & 0.0156 & 0.00509 & 0.000785 & 0.000504 & 0.00464 \end{bmatrix} \quad (37)$$

$$A2 - Cyx_{h44} = \begin{bmatrix} & \#1B & \#2B & \#3B & \#4B & \#5B & \#6B & \#7B & \#8B \\ \#14P & 0.0209 & 0.00251 & 0.0692 & 0.0168 & 0.00240 & 1.73 & 23.4 & 1.08 \\ \#29P & 0.064 & 0.000460 & 0.0318 & 0.00500 & 0.00187 & 2.25 & 12.6 & 42.2 \\ \#31P & 0.405 & 0.00125 & 0.0324 & 0.00657 & 0.00408 & 3.33 & 19.4 & 50.6 \\ \#49P & 0.234 & 0.000523 & 0.0371 & 1.43 \times 10^{-5} & 9.84 \times 10^{-6} & 0.00672 & 0.0443 & 0.312 \\ \#51P & 1.87 & 0.00384 & 0.0735 & 1.67 \times 10^{-5} & 7.89 \times 10^{-6} & 0.00113 & 0.00849 & 0.560 \\ \#69P & 6.88 & 0.168 & 1.28 & 0.000406 & 5.18 \times 10^{-5} & 6.56 \times 10^{-5} & 0.000424 & 0.00283 \\ \#81P & 125 & 0.357 & 0.509 & 0.000512 & 0.000248 & 0.000111 & 0.000196 & 0.00401 \\ \#89P & 1.35 & 0.753 & 1.86 & 0.00413 & 0.00346 & 0.000955 & 0.00219 & 0.00237 \end{bmatrix} \quad (38)$$

where $A2 - Kxx_{g44}$, $A2 - Kyy_{g44}$, $A2 - Cxx_{g44}$, $A2 - Cyy_{g44}$,$A2 - Kxy_{g44}$, $A2 - Kyx_{g44}$, $A2 - Cxy_{g44}$ and $A2 - Cyx_{g44}$ are the matrices of the maximum identification error of the main stiffness coefficient in the x direction, the main stiffness coefficient in the y direction, the main damping coefficient in the x direction, the main damping coefficient in the y direction, the cross-coupled stiffness coefficient in the x direction, the cross-coupled stiffness coefficient in the y direction, the cross-coupled damping coefficient in the x direction and the cross-coupled damping coefficient in the y direction of #1 to #8 bearings under different last measuring point conditions in the simulation of h4.4 using Algorithm II; the red numbers show the best identification results when the last measuring point is changed.

Table 2. The last measuring point.

#14	#29	#31	#49	#51	#69	#71	#89

3.2.2. Discussion

In the first kind of numerical simulation, the unbalance responses calculated by CR-DAM are directly put into Algorithm I and Algorithm II to identify the bearing coefficients.

In the simulation of g4.4 based on Algorithm I, the relative identification errors of #1 bearing's main coefficients are almost equal to zero, while the identification errors of other bearings can be very big when #14 node near #1 bearing is used as the last measuring point. Moreover, when #29 node (near #2 bearing), #33 (near #3 bearing), #49 (near #4 bearing), #53 (near #5 bearing), #69 (near #6 bearing), #73 (near #7 bearing) and #91 (near #8 bearing) are used as the last measuring points, respectively, the relative identification errors of #2, #3, #4, #5, #6, #7 and #8 bearing's main coefficients are almost equal to zero, respectively.

Moreover, the same rule can be obtained according to the simulation results of g4.4 and h4.4 based on Algorithm II. It is indicated that the measuring points in Tables 1 and 2 can adjust the identification error. If the measuring point is near a bearing, the identification accuracy of the bearing is high. Hence, the points in Tables 1 and 2 are called adjustment points.

In addition, the identification errors of main stiffness coefficients are smaller than that of the main damping coefficients in the simulation based on Algorithm I. This is because the main stiffness coefficients are far greater than the main damping coefficients for a rolling bearing. The numerical calculation errors of computers, such as rounding error and calculation accuracy, have little influence on big numbers and a great influence on small numbers.

In the simulations of g4.4 based on Algorithm II, the identification errors of main stiffness coefficients are also smaller than that of the main damping coefficients. It is also because the main stiffness coefficients are much bigger than the main damping coefficients, and the numerical calculation errors have little influence on big numbers and a great influence on small numbers. However, the identification errors of cross-coupled stiffness coefficients are bigger than that of the cross-coupled damping coefficients. The cross-coupled stiffness and damping coefficients are equal and are nearly zero in g4.4. This indicates that when the difference between the cross-coupled stiffness coefficient and cross-coupled damping coefficient is small, the identification errors of the cross-coupled stiffness coefficients are bigger than those of the cross-coupled damping coefficients.

Similarly, the identification errors of damping coefficients are also smaller than those of the stiffness coefficients in the simulation of h4.4 based on Algorithm II. This is because the difference between the stiffness coefficients and damping coefficients is not particularly big. It can be inferred that the damping coefficients of journal bearings can be better identified than the stiffness coefficients by using Algorithm II.

3.3. Application of Adjustment Point

3.3.1. Results

Results of the First Kind of Simulation

(1) Simulation results based on Algorithm I.

In this simulation, the computational examples are g1.1 and g1.4. The adjustment points in Tables 3 and 4 are considered. Tables 5 and 6, which show the maximum relative errors of identified coefficient of each bearing's main stiffness coefficients and main damping coefficients, are obtained.

Table 3. The measuring points for g1.1.

The m + n measuring points	#15 (#1 bearing)	#90 (#2 bearing)	#61 (#disc)
Adjustment point	#14	#91	

Table 4. The measuring points for g1.4.

The m + n measuring points	#15 (#1 bearing)	#90 (#2 bearing)	#21 (disc)	#41 (disc)	#61 (disc)	#81 (disc)
Adjustment point	#14	#91				

Table 5. The biggest relative error of the identified main coefficients, based on Algorithm I and g1.1.

Relative error	k1.xx	k2.xx	c1.xx	c2.xx	k1.yy	k2.yy	c1.yy	c2.yy
(%)	2.706×10^{-7}	6.16×10^{-8}	0.0306	0.00977	2.39×10^{-7}	8.162×10^{-8}	0.141	0.0175

Table 6. The biggest relative error of the identified main coefficients based on Algorithm I and g1.4.

Relative error	k1.xx	k2.xx	c1.xx	c2.xx	k1.yy	k2.yy	c1.yy	c2.yy
(%)	4.11×10^{-7}	8.13×10^{-8}	0.0227	0.00204	1.24×10^{-7}	5.31×10^{-8}	0.0130	0.00834

For g1.1, according to Table 5, the maximum relative errors of the two bearings' main coefficients are almost equal to zero. The maximum relative errors of k1.xx, k1.yy, k2.xx and k2.yy are only 2.71×10^{-7}%, 6.16×10^{-8}%, 2.39×10^{-7}% and 8.16×10^{-8}%, respectively. Moreover, the maximum relative errors of c1.xx, c1.yy, c2.xx and c2.yy, which are 0.0306%, 0.00977%, 0.141% and 0.0175%, respectively, almost equal zero; although, they are bigger than those of the main stiffness coefficients.

For g1.4, according to Table 6, the maximum relative errors of the two bearings' main coefficients are almost equal to zero. They are only 4.11×10^{-7}%, 8.13×10^{-8}%, 0.0227%, 0.00204%, 1.24×10^{-7}%, 5.31×10^{-8}%, 0.0130% and 0.00834%, respectively. Moreover, the identification errors of the main stiffness coefficients are smaller than those of the main damping coefficients.

(2) Simulation results based on Algorithm II.

Simulations considering adjustment points shown in Tables 3, 4, 7 and 8 are conducted using g1.1, g1.4, h1.1 and h1.4, respectively. Tables 9–12 show the maximum relative errors of identified coefficients of each bearing obtained. The results are the following.

Table 7. The measuring points for h1.1.

The m + n measuring points	#3 (#1 bearing)	#47 (#2 bearing)	#31 (#disc)
Adjustment point	#2	#48	

Table 8. The measuring points for h4.4.

The m + n measuring points	#3 (#1 bearing)	#47 (#2 bearing)	#21 (disc)	#41 (disc)	#61 (disc)	#81 (disc)
Adjustment point	#2	#48				

Table 9. The biggest relative identification errors of main coefficients and the maximum identified absolute value of cross-coupled coefficients using g1.1.

Relative error	k1.xx	k2.xx	c1.xx	c2.xx	k1.yy	k2.yy	c1.yy	c2.yy
(%)	3.25×10^{-7}	6.00×10^{-7}	0.00573	0.00192	3.11×10^{-7}	5.63×10^{-7}	0.0287	0.00352
Identified absolute	k1.xy	k2.xy	c1.xy	c2.xy	k1.yx	k2.yx	c1.yx	c2.yx
value	0.0333	0.0108	0.00998	0.00108	0.117	0.0159	0.00888	0.00155

Table 10. The biggest relative identification error of main coefficients and the maximum identified absolute value of cross-coupled coefficients using g1.4.

Relative error	k1.xx	k2.xx	c1.xx	c2.xx	k1.yy	k2.yy	c1.yy	c2.yy
(%)	4.94×10^{-7}	1.85×10^{-7}	0.00472	0.000425	2.22×10^{-7}	9.48×10^{-8}	0.00278	0.00170
Identified absolute	k1.xy	k2.xy	c1.xy	c2.xy	k1.yx	k2.yx	c1.yx	c2.yx
value	0.0210	0.00870	0.0154	0.00145	0.0108	0.00762	0.00480	0.000967

Table 11. The biggest relative identification error using h1.1.

Relative error	k1.xx	k2.xx	k1.yy	k2.yy	k1.xy	k2.xy	k1.yx	k2.yx
(%)	0.00435	0.00350	0.00537	0.0118	0.0324	0.0218	0.00346	0.00633
Relative error	c1.xx	c2.xx	c1.yy	c2.yy	c1.xy	c2.xy	c1.yx	c2.yx
(%)	1.56×10^{-5}	0.000229	2.45×10^{-5}	0.000204	0.000416	0.000188	9.41×10^{-5}	0.000190

Table 12. The biggest relative identification error using h1.4.

Relative error	k1.xx	k2.xx	k1.yy	k2.yy	k1.xy	k2.xy	k1.yx	k2.yx
(%)	0.0535	0.0367	0.0184	0.181	0.677	0.241	0.0131	0.0879
Relative error	c1.xx	c2.xx	c1.yy	c2.yy	c1.xy	c2.xy	c1.yx	c2.yx
(%)	0.000281	0.000627	0.000152	0.000612	0.00926	0.000473	0.000265	0.000604

For g1.1, according to Table 9, the maximum relative errors of the two bearings' main coefficients, which are only 3.25×10^{-7}%, 6.00×10^{-7}%, 0.00573%, 0.00192%, 3.11×10^{-7}%, 5.63×10^{-7}%, 0.0287% and 0.00352%, respectively, are also quite small. Moreover, the identification errors of the main stiffness coefficients are smaller than those of the main damping coefficients. For the cross-coupled coefficients of the two bearings, the absolute identified values are only 0.0333, 0.0108, 0.00998, 0.00108, 0.117, 0.0159, 0.00887 and 0.00155, respectively. They are almost equal to zero.

For g1.4, according to Table 10, the maximum relative errors of the two bearings' main coefficients, which are only 4.94×10^{-7}%, 1.85×10^{-7}%, 0.00472%, 0.000425%, 2.22×10^{-7}%, 9.48×10^{-8}%, 0.00278% and 0.00170%, respectively, are also quite small. Moreover, the identification errors of the main stiffness coefficients are smaller than those of the main damping coefficients. For the cross-coupled coefficients of the two bearings, the absolute identified values are only 0.0210, 0.00870, 0.0154, 0.00145, 0.0108, 0.00762, 0.00480 and 0.000967, respectively. They are almost equal to zero.

For h1.1, according to Table 11, the maximum relative errors of the two bearings' stiffness coefficients are almost equal to zero. They are 0.00435%, 0.00350%, 0.00537%, 0.0118%, 0.0324%, 0.0218%, 0.00346% and 0.00633%, respectively. Moreover, the maximum relative errors of the two bearings' damping coefficients, which are only 1.56×10^{-5}%, 0.000229%, 2.45×10^{-5}% and 0.000204%, 0.000416%, 0.000188%, 9.41×10^{-5}% and 0.000190%, respectively, are smaller than those of the stiffness coefficients.

For h1.4, according to Table 12, the maximum relative errors of the two bearings' stiffness coefficients are almost equal to zero. They are 0.0535%, 0.0367%, 0.01841841%, 0.181%, 0.677%, 0.241% and 0.0131%, 0.0880%, respectively. Moreover, the maximum relative errors of the two bearings' damping coefficients, which are only 0.000281%, 0.000627%, 0.000152%, 0.0006124%, 0.00926%, 0.000473%, 0.000265% and 0.000604%, respectively, are smaller than those of the stiffness coefficients.

Results of the Second Kind of Simulation

(1) Simulation results based on Algorithm I.

The proposed adjustment points are applied in the second kind of simulation. Figure 4, which represents the maximum identified relative errors of each bearing's main coefficients, is obtained using g4.4. The points in Table 1 are used as adjustment points.

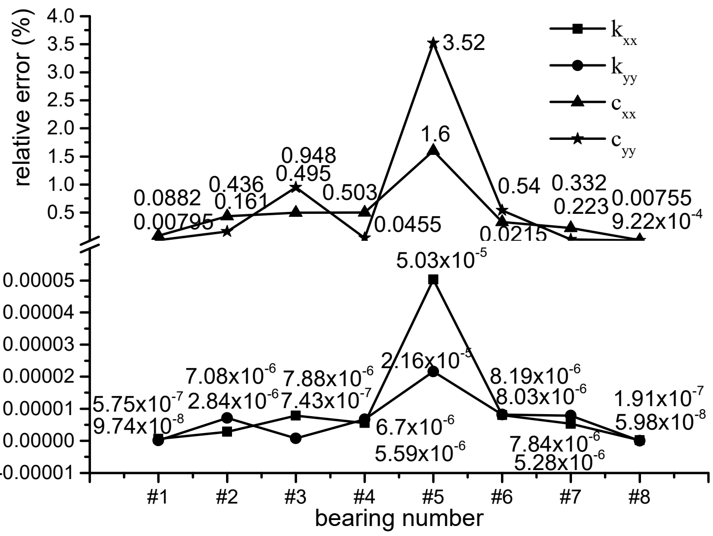

Figure 4. The biggest relative identification error obtained using g4.4 based on Algorithm I.

For g4.4, according to Figure 4, the maximum relative errors of k1.xx, k2.xx, ..., k8.xx are almost equal to zero. They are only 5.75×10^{-7}%, 2.84×10^{-6}%, 7.88×10^{-6}%, 5.59×10^{-6}%, 5.03×10^{-5}%, 8.03×10^{-6}%, 5.28×10^{-6}% and 1.91×10^{-7}%, respectively. The maximum relative errors of c1.xx, c2.xx, ..., c8.xx, which are only 0.0882%, 0.436%, 0.495%, 0.503%, 1.60%, 0.332%, 0.223% and 0.00755%, respectively, are bigger than that of the main stiffness coefficients in the x direction. However, they are quite small. Moreover, the maximum relative errors of k1.yy, k2.yy, ..., k8.yy are only 9.74×10^{-8}%, 7.08×10^{-6}%, 7.43×10^{-7}%, 6.70×10^{-6}%, 2.16×10^{-5}%, 8.19×10^{-6}%, 7.84×10^{-6}% and 5.98×10^{-8}%, respectively. They are also almost equal to zero. The maximum relative errors of c1.yy, c2.yy, ..., c8.yy are very small, but are bigger than that of the stiffness coefficients in the y direction. They are only 0.00795%, 0.161%, 0.948%, 0.0455%, 3.52%, 0.540%, 0.0215% and 0.000922%, respectively.

Tables 13 and 14, which represent the maximum identified relative errors of each bearing's main coefficients, are obtained in the second kind simulations of g1.4 and g1.1. The nodes in Tables 3 and 4 are used as adjustment points. Similar rules can be obtained according to Tables 13 and 14.

Table 13. The biggest relative identification error using the computational example g1.4.

Relative error	k1.xx	k2.xx	c1.xx	c2.xx	k1.yy	k2.yy	c1.yy	c2.yy
(%)	4.11×10^{-7}	8.13×10^{-8}	0.0227	0.00204	1.24×10^{-7}	5.31×10^{-8}	0.0130	0.00834

Table 14. The biggest relative identification error using the computational example g1.1.

Relative error	k1.xx	k2.xx	c1.xx	c2.xx	k1.yy	k2.yy	c1.yy	c2.yy
(%)	2.71×10^{-7}	6.16×10^{-8}	0.0306	0.00977	2.39×10^{-7}	8.16×10^{-8}	0.141	0.0175

(2) Simulation results based on Algorithm II.

Figure 5, which shows the maximum relative errors of each bearing's main coefficients and the absolute value of each bearing's cross-coupled coefficients, is obtained using g4.4. The nodes, where the bearings and discs are located, are used as the m + n measuring points in these simulations. The adjustment points shown in Table 1 are used.

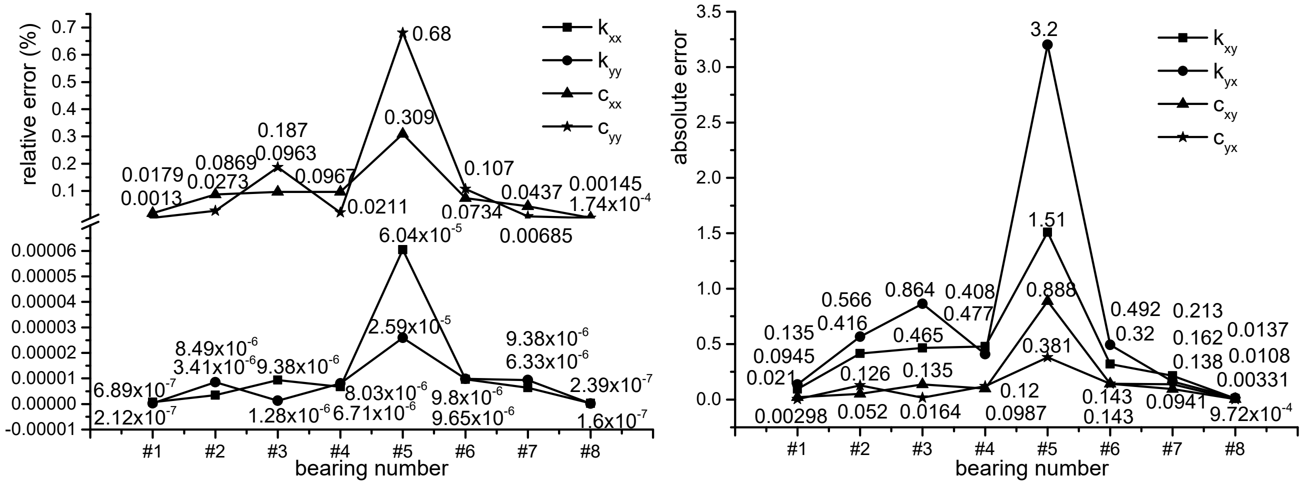

Figure 5. The biggest identification error obtained using g4.4 based Algorithm II.

According to Figure 5, for the main coefficients, the maximum relative errors of k1.xx, k2.xx, . . . , k8.xx are almost equal to zero. They are only 6.89×10^{-7}%, 3.41×10^{-6}%, 9.38×10^{-6}%, 6.71×10^{-6}%, 6.04×10^{-5}%, 9.65×10^{-6}%, 6.33×10^{-6}% and 2.39×10^{-7}%, respectively. The maximum relative errors of c1.xx, c2.xx, . . . , c8.xx are bigger than that of the stiffness coefficients. They are 0.0179%, 0.0869%, 0.0963%, 0.0967%, 0.309%, 0.0734%, 0.0437% and 0.00145%, respectively, and are quite small. In the y direction, the maximum relative errors of k1.yy, k2.yy, . . . , k8.yy are only 2.12×10^{-7}%, 8.49×10^{-6}%, 1.28×10^{-6}%, 8.03×10^{-6}%, 2.59×10^{-5}%, 9.80×10^{-6}%, 9.38×10^{-6}% and 1.60×10^{-7}%, respectively. The maximum relative errors of the identified c1.yy, c2.yy, . . . , c8.yy, which are only 0.00130%, 0.0273%, 0.187%, 0.0211%, 0.680%, 0.107%, 0.00685% and 0.000174%, respectively, are also very small; though, they are bigger than that of the stiffness coefficients.

For the cross-coupled coefficients, the identified values are almost equal to zero (the setting value) and the identification errors of the cross-coupled stiffness coefficients are higher than those of the cross-coupled damping coefficients. The maximum absolute values of k1.xy, k2.xy, . . . , k8.xy are only 0.0945, 0.416, 0.465, 0.477, 1.51, 0.320, 0.213 and 0.0108, respectively. The maximum absolute values of c1.xy, c2.xy, . . . , c8.xy are only 0.0210, 0.0520, 0.135, 0.0987, 0.888, 0.143, 0.0941 and 0.00331, respectively. The maximum absolute values of k1.yx, k2.yx, . . . , k8.yx are only 0.135, 0.566, 0.864, 0.408, 3.20, 0.492, 0.162 and 0.0137, respectively. The maximum absolute values of the identified c1.yx, c2.yx, . . . , c8.yx are only 0.00298, 0.126, 0.0164, 0.120, 0.381, 0.143, 0.138 and 0.000972, respectively.

Similar results can be obtained according to Tables 15 and 16, which show the simulation results of g1.4 and g1.1.

Table 15. The biggest identification error using the computational example g1.4.

Relative error (%)	k1.xx 4.94×10^{-7}	k2.xx 1.11×10^{-7}	c1.xx 0.00472	c2.xx 0.000425	k1.yy 1.51×10^{-7}	k2.yy 9.51×10^{-8}	c1.yy 0.00278	c2.yy 0.00170
Identified absolute value	k1.xy 0.0210	k2.xy 0.00870	c1.xy 0.0154	c2.xy 0.00145	k1.yx 0.0108	k2.yx 0.00762	c1.yx 0.00480	c2.yx 0.000967

Table 16. The biggest identification error using the computational example g1.1.

Relative error (%)	k1.xx 3.25×10^{-7}	k2.xx 1.70×10^{-7}	c1.xx 0.00573	c2.xx 0.00192	k1.yy 3.12×10^{-7}	k2.yy 5.40×10^{-7}	c1.yy 0.0287	c2.yy 0.00352
Identified absolute value	k1.xy 0.0333	k2.xy 0.0108	c1.xy 0.00998	c2.xy 0.00108	k1.yx 0.117	k2.yx 0.0159	c1.yx 0.00888	c2.yx 0.00155

Using the rotor h4.4 supported by oil-journal bearings, the maximum relative errors of each bearing's main and cross-coupled coefficients are obtained in Figure 6. The nodes, where the bearings and discs are located, are used as the m + n measuring points in these simulations. The adjustment points in Table 2 are used.

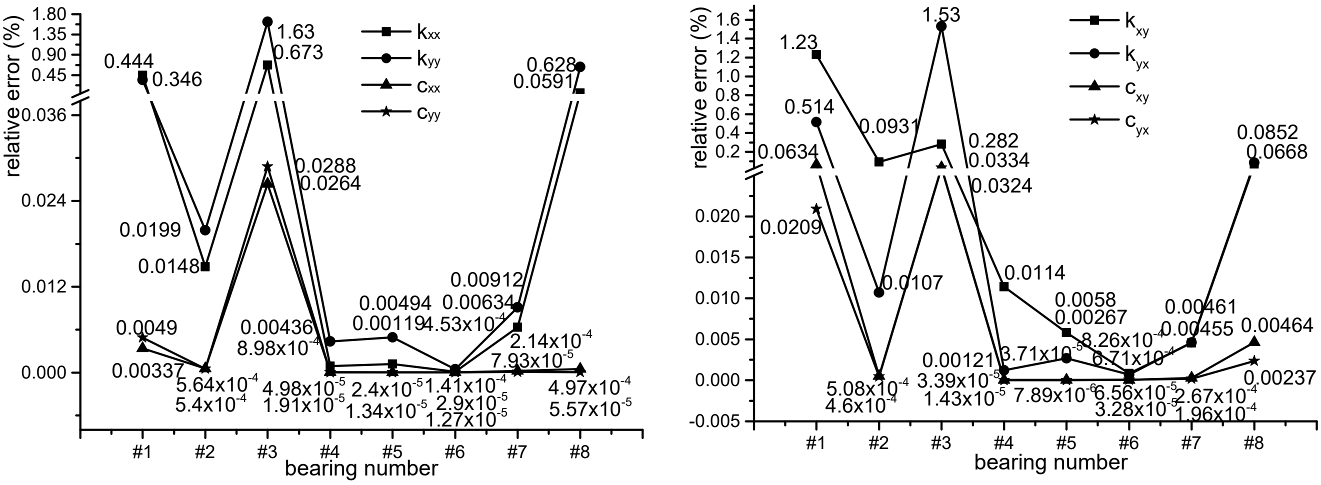

Figure 6. The biggest identification error obtained using h'4.4 based on Algorithm II.

According to Figure 6, for the main coefficients, the maximum relative errors of k1.xx, k2.xx, . . . , k8.xx are almost equal to zero. They are only 0.444%, 0.0148%, 0.673%, 0.000898%, 0.00119%, 0.000141%, 0.00634% and 0.0591%, respectively. The maximum relative errors of c1.xx, c2.xx, . . . , c8.xx are smaller than those of the stiffness coefficients. They are 0.00337%, 0.000564%, 0.0264%, 4.98×10^{-5}%, 2.40×10^{-5}%, 1.27×10^{-5}%, 0.000214% and 0.000497%, respectively, and are quite small. In the y direction, the maximum relative errors of k1.yy, k2.yy, . . . , k8.yy are only 0.346%, 0.0199%, 1.63%, 0.00436%, 0.00494%, 0.000453%, 0.00912% and 0.628%, respectively. The maximum relative errors of the identified c1.yy, c2.yy, . . . , c8.yy, which are only 0.00490%, 0.000540%, 0.0288%, 1.91×10^{-5}%, 1.34×10^{-5}%, 2.90×10^{-5}%, 7.93×10^{-5}% and 5.57×10^{-5}%, respectively, are smaller than that of the stiffness coefficients.

For the cross-coupled coefficients, the identification errors are almost equal to zero and the identification errors of the cross-coupled stiffness coefficients are higher than those of the cross-coupled damping coefficients. The maximum relative errors of k1.xy, k2.xy, . . . , k8.xy are only 1.23%, 0.0931%, 0.282%, 0.0114%, 0.00580%, 0.000826%, 0.00455% and 0.0668%, respectively. The maximum relative errors of c1.xy, c2.xy, . . . , c8.xy are only 0.0634%, 0.000508%, 0.0334%, 3.39×10^{-5}%, 3.71×10^{-5}%, 3.28×10^{-5}%, 0.000267% and 0.00464%, respectively. The maximum relative errors of k1.yx and k2.yx, . . . , k8.yx are 0.514%, 0.0107%, 1.53%, 0.00121%, 0.00267%, 0.000671%, 0.00461% and 0.0852%, respectively. The maximum relative errors of c1.yx and c2.yx, . . . , c8.yx are only 0.0209%, 0.000460%, 0.0324%, 1.43×10^{-5}%, 7.89×10^{-6}%, 6.56×10^{-5}%, 0.000196% and 0.00237%, respectively.

Similar results can be obtained according to Tables 17 and 18, which show the simulations results of h1.4 and h1.1.

Table 17. The biggest identification error using the computational example h1.4.

Relative error	k1.xx	k2.xx	c1.xx	c2.xx	k1.yy	k2.yy	c1.yy	c2.yy
(%)	0.0535	0.0373	0.000281	0.000620	0.0184	0.182	0.000152	0.000618
Relative error	k1.xy	k2.xy	c1.xy	c2.xy	k1.yx	k2.yx	c1.yx	c2.yx
(%)	0.677	0.2494	0.00926	0.000472	0.0131	0.0857	0.000265	0.000627

Table 18. The biggest identification error using the computational example h1.1.

Relative error	k1.xx	k2.xx	c1.xx	c2.xx	k1.yy	k2.yy	c1.yy	c2.yy
(%)	0.00435	0.00350	1.56×10^{-5}	0.000229	0.00537	0.0118	2.45×10^{-5}	0.000204
Relative error	k1.xy	k2.xy	c1.xy	c2.xy	k1.yx	k2.yx	c1.yx	c2.yx
(%)	0.0324	0.0218	0.000416	0.000188	0.00345	0.00633	9.41×10^{-5}	0.000190

3.3.2. Discussion

From the above, the identification errors are almost equal to zero when the set error is zero by using the proposed adjustment point. Moreover, the identification errors are also almost equal to zero; although, the set measured error is (5%, 5°). This indicates that if the errors of all measured unbalance responses are equal, the bearing coefficients will be identified accurately. Therefore, the repeatability precision of each measuring channel of the unbalance response measurement system is very important for Algorithm I and Algorithm II.

In addition, when the two methods are used for rolling bearings, the identification errors of the main stiffness coefficients are smaller than those of the main damping coefficients. While for the cross-coupled coefficients, the identification errors of the cross-coupled stiffness coefficients are higher than that of the cross-coupled damping coefficients. When Algorithm II is used for oil journal bearings, the identification errors of the main stiffness coefficients are bigger than those of the main damping coefficients. Moreover, the identification errors of the cross-coupled stiffness coefficients are bigger than those of the cross-coupled damping coefficients. Hence, for Algorithm II used for rolling bearings, the stiffness coefficients of rolling bearings can be better identified than the damping coefficients. Whereas, when Algorithm II is used for journal bearings, the damping coefficients can be better identified than the stiffness coefficients. The reason is that the numerical calculation errors of computers, such as rounding error and calculation accuracy, have little influence on big numbers and a great influence on small numbers.

3.4. Effect of Sensor Resolution

3.4.1. Results

The unbalance responses calculated by CRDAM contaminating three kinds of typical sensor resolution, which are 0.1 mn, 1 nm, and 1 um, respectively, are the input data to the two algorithms. The adjustment points are in Tables 1 and 2. Figures 7–9 are obtained. Figure 7 is the statistical results of the amount of LEFPs of the identified main coefficients of g4.4 based on Algorithm I. Figures 8 and 9 are the statistical results of the amount of LEFPs of the identified main coefficients of g4.4 and h4.4 based on Algorithm II.

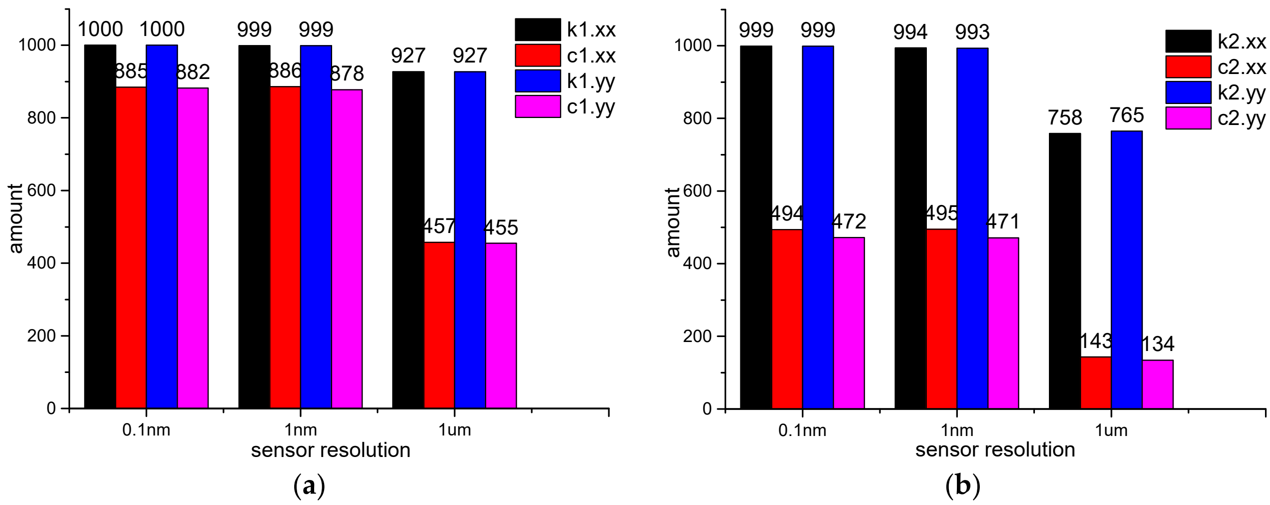

Figure 7. *Cont.*

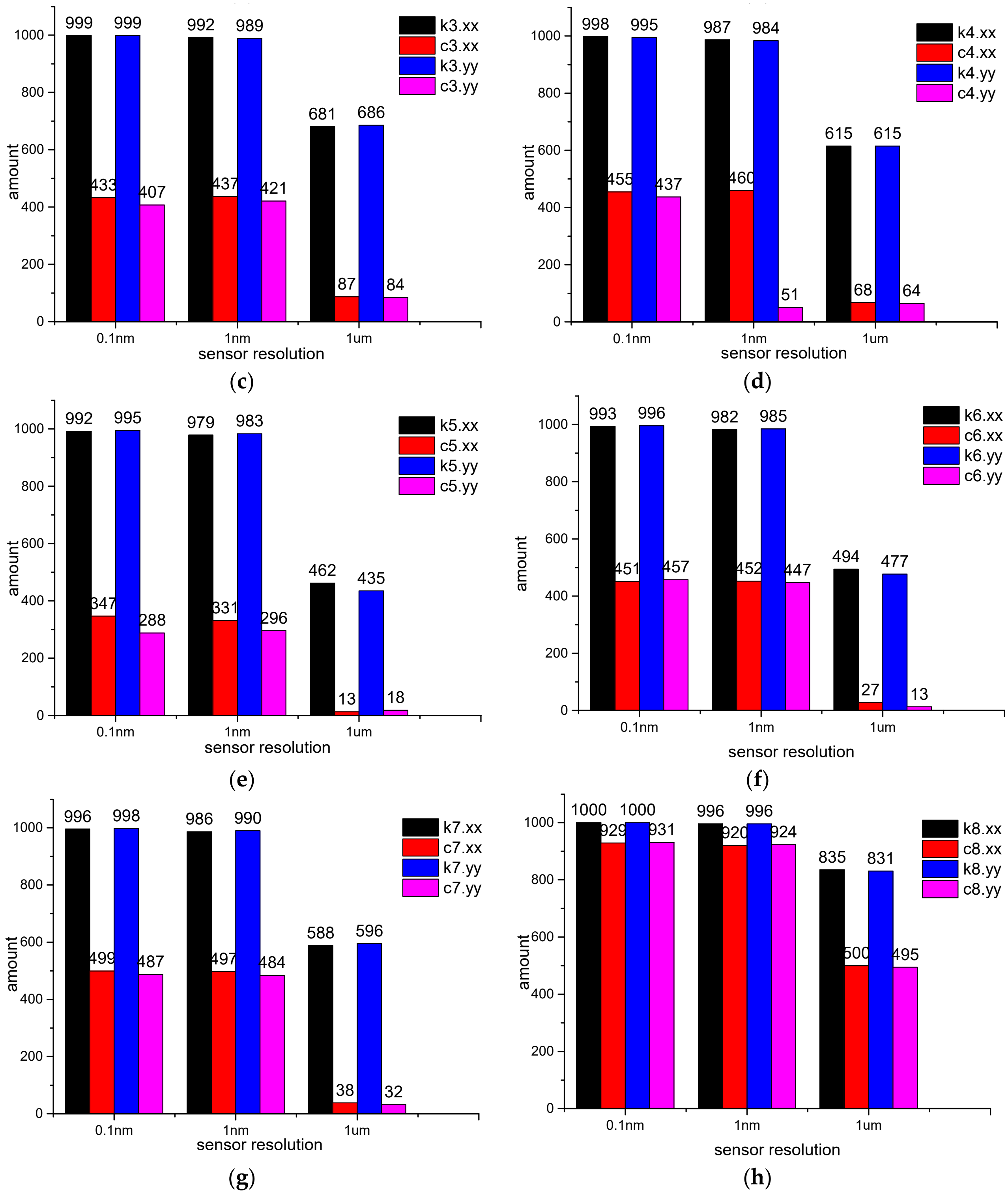

Figure 7. Statistical results of the amount of the frequencies, at which the related error is less than 10%: (**a**) #1 bearing; (**b**) #2 bearing; (**c**) #3 bearing; (**d**) #4 bearing; (**e**) #5 bearing; (**f**) #6 bearing; (**g**) #7 bearing; (**h**) #8 bearing.

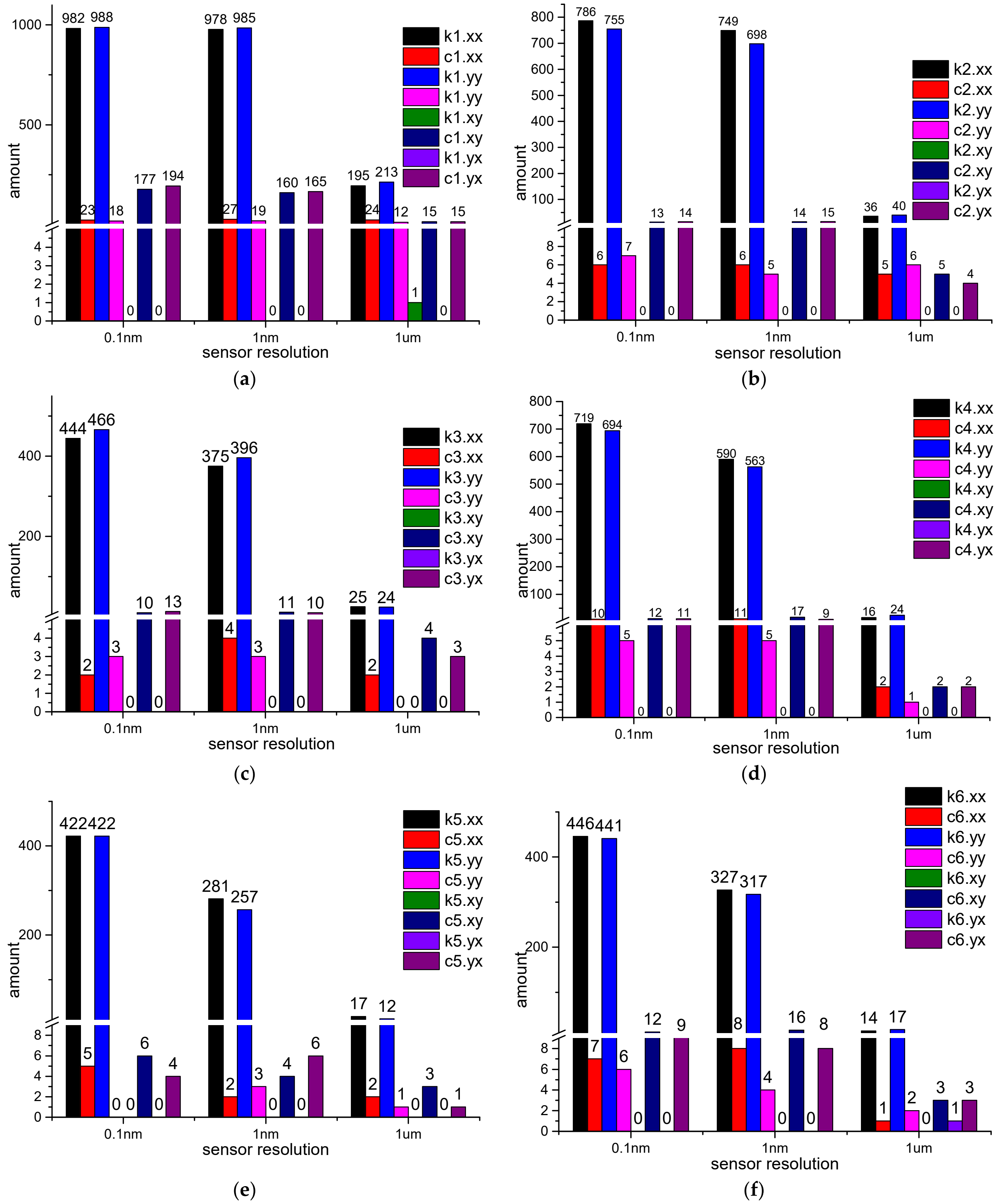

Figure 8. *Cont.*

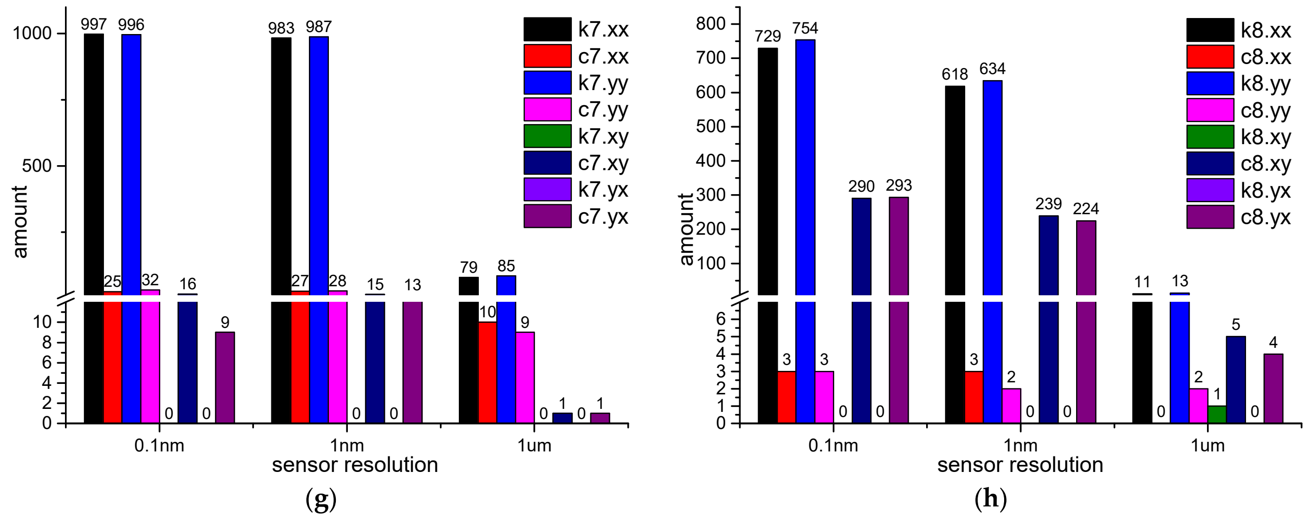

Figure 8. Statistical results of the amount of the frequencies, at which the related error is less than 10% or the absolute value is less than 10: (**a**) #1 bearing; (**b**) #2 bearing; (**c**) #3 bearing; (**d**) #4 bearing; (**e**) #5 bearing; (**f**) #6 bearing; (**g**) #7 bearing; (**h**) #8 bearing.

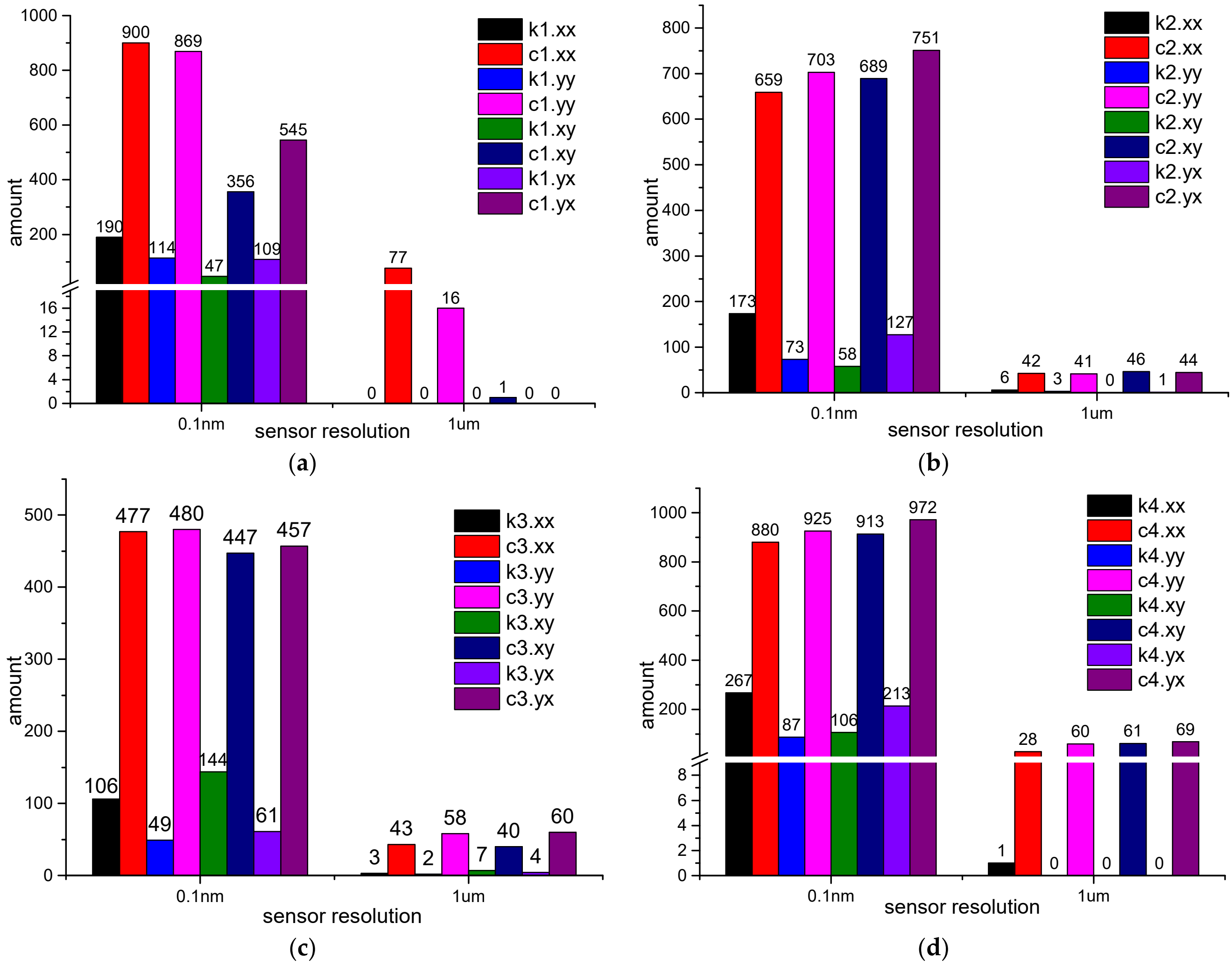

Figure 9. *Cont.*

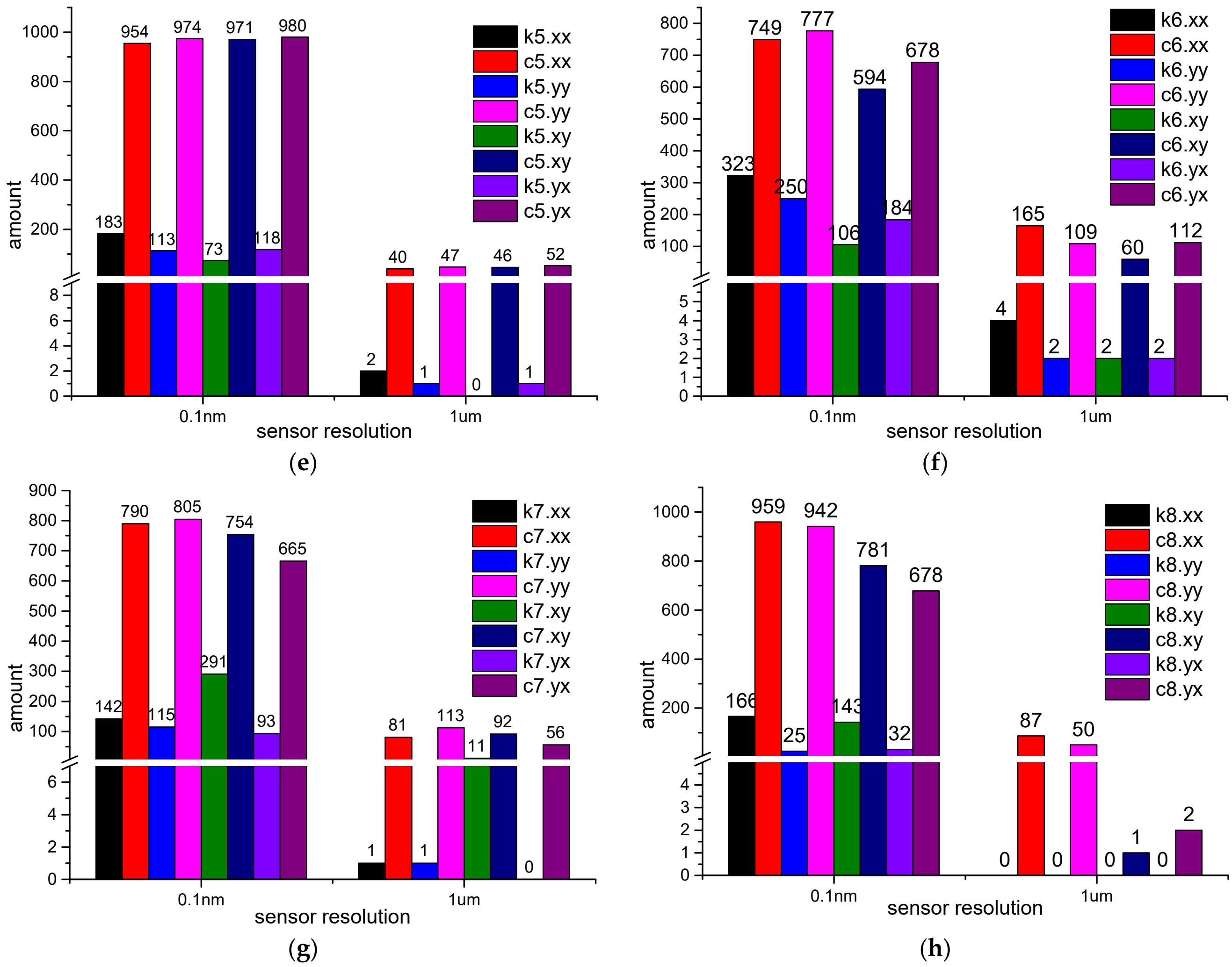

Figure 9. Statistical results of the amount of the frequencies, at which the related error is less than 10% or the absolute value is less than 10: (**a**) #1 bearing; (**b**) #2 bearing; (**c**) #3 bearing; (**d**) #4 bearing; (**e**) #5 bearing; (**f**) #6 bearing; (**g**) #7 bearing; (**h**) #8 bearing.

Simulations Results Based on Algorithm I

According to Figure 7, the following can be obtained.

(1) 0.1 nm resolution.

Most identification errors of the main stiffness coefficients are smaller than 10% and there are some identification errors of the main damping coefficients smaller than 10%.

In the x direction, the amounts of LEFPs of k1.xx, k2.xx, . . . , k8.xx are 1000, 999, 999, 998, 992, 993, 996 and 1000, respectively. While for c1.xx, c2.xx, . . . , c8.xx, the amounts are 885, 494, 433, 455, 347, 451, 499 and 929, respectively. In the y direction, there are 1000, 999, 999, 995, 995, 996, 998 and 1000 LEFPs of k1.yy, k2.yy, . . . , k8.yy, respectively. While for c1.yy, c2.yy, . . . , c8.yy, the amounts are 882, 472, 407, 437, 288, 457, 487 and 931, respectively.

(2) 1 nm resolution.

Most identification errors of the main stiffness coefficients are smaller than 10%. Some identification errors are smaller than 10% for the main damping coefficients.

In the x direction, the amounts of LEFPs of k1.xx, k2.xx, . . . , k8.xx are 999, 994, 992, 987, 979, 982, 986 and 996, respectively. While for c1.xx, c2.xx, . . . , c8.xx, the amounts are 886, 495, 437, 460, 331, 452, 497 and 920, respectively. In the y direction, there are 999, 993, 989, 984, 983, 985, 990 and 996 LEFPs of k1.yy, k2.yy, . . . , k8.yy, respectively. While for c1.yy, c2.yy, . . . , c8.yy, the amounts are 878, 471, 421, 51, 296, 447, 484 and 924, respectively.

(3) 1 um resolution.

Most identification errors of the main stiffness coefficients are smaller than 10%. While for the main damping coefficients, only some identification errors are smaller than 10%.

In the x direction, the amounts of LEFPs of k1.xx, k2.xx, . . . , k8.xx are 927, 758, 681, 615, 462, 494, 588 and 835, respectively. While for c1.xx, c2.xx, . . . , c8.xx, the amounts are 457, 143, 87, 68, 13, 27, 38 and 500, respectively. In the y direction, there are 927, 765, 686, 615, 435, 477, 596 and 831 LEFPs of k1.yy, k2.yy, . . . , k8.yy, respectively. While for c1.yy, c2.yy, . . . , c8.yy, the amounts are 455, 134, 84, 64, 18, 13, 32 and 495, respectively.

Other simulations results are obtained as follows.

(1) The maximum relative error of the identified coefficient is very big and it appears at low frequency.
(2) The main stiffness coefficients cannot be identified at 1 Hz when 1 nm resolution is used and the main stiffness coefficients cannot be identified from 1 to 33 Hz when 1 um resolution is applied.

Similar results can be obtained from the simulations of g1.4 and g1.1, whose results are shown in Figures A1–A8 in Appendix A.

Simulations Results Based on Algorithm II

According to Figure 8, the following can be obtained.

(1) 0.1 nm resolution.

Most of the identification errors of the main stiffness coefficients are smaller than 10%, but there are only several identification errors smaller than 10% for the main damping coefficients.

In the x direction, the amounts of LEFPs of k1.xx, k2.xx, . . . , k8.xx are 982, 786, 444, 719, 422, 446, 729 and 997, respectively. While for c1.xx, c2.xx, . . . , c8.xx, the amounts are only 23, 6, 2, 10, 5, 7, 3 and 25, respectively. In the y direction, there are 988, 755, 466, 694, 422, 441, 754 and 996 LEFPs of k1.yy, k2.yy, . . . , k8.yy, respectively. While for c1.yy, c2.yy, . . . , c8.yy, the amounts are only 18, 7, 3, 5, 0, 6, 3 and 32, respectively.

As for the cross-coupled stiffness coefficients in the x direction, there is no one LEFP of k1.xy, k2.xy, . . . , k8.xy, whereas there are a few LEFPs of c1.xy, c2.xy, . . . , c8.xy. The amounts are 177, 13, 10, 12, 6, 12, 16 and 290, respectively. In the y direction, the amounts of LEFPs of k1.yx, k2.yx, . . . , k8.yx are all zero. However, there are some LEFPs of c1.yx, c2.yx, . . . , c8.yx, whose numbers are 194, 14, 13, 11, 4, 9, 9 and 293, respectively.

(2) 1 nm resolution.

For the main stiffness coefficients, there are many identification errors smaller than 10%. While for the main damping coefficients, only several identification errors are smaller than 10%.

In the x direction, the amounts of LEFPs of k1.xx, k2.xx, . . . , k8.xx are 978, 749, 375, 590, 281, 327, 618 and 983, respectively. While for c1.xx, c2.xx, . . . , c8.xx, the amounts are only 27, 6, 4, 11, 2, 8, 3 and 27, respectively. In the y direction, there are 985, 698, 396, 563, 257, 317, 634 and 987 LEFPs of k1.yy, k2.yy, . . . , k8.yy, respectively. While for c1.yy, c2.yy, . . . , c8.yy, the amounts are only 19, 5, 3, 5, 3, 4, 2 and 28, respectively.

As for the cross-coupled stiffness coefficients in the x direction, there is no one LEFP of k1.xy, k2.xy, . . . , k8.xy, whereas there are a few low error frequency points of c1.xy, c2.xy, . . . , c8.xy. The amounts are 160, 14, 11, 17, 4, 16, 15 and 239, respectively. In the y direction, the numbers of LEFPs of k1.yx, k2.yx, . . . , k8.yx are all zero. However, there are some LEFPs of c1.yx, c2.yx, . . . , c8.yx, whose numbers are 165, 15, 10, 9, 6, 8, 13 and 224, respectively.

(3) 1 um resolution.

There are only some identification errors of the main stiffness coefficients smaller than 10% and several identification errors of the main damping coefficients are bigger than 10%.

In the x direction, the amounts of LEFPs of k1.xx, k2.xx, . . . , k8.xx are 195, 36, 25, 16, 17, 14, 11 and 79 and 983, respectively. While for c1.xx, c2.xx, . . . , c8.xx, the amounts are only 24, 5, 2, 2, 2, 1, 0 and 10, respectively. In the y direction, there are 213, 40, 24, 24, 12, 17, 13 and 85 LEFPs of k1.yy, k2.yy, . . . , k8.yy, respectively. While for c1.yy, c2.yy, . . . , c8.yy, the numbers are only 12, 6, 0, 1, 1, 2, 2 and 9, respectively.

As for the cross-coupled stiffness coefficients in the x direction, the LEFPs of k1.xy, k2.xy, . . . , k8.xy are 0, 0, 0, 0, 0, 0, 0 and 1, respectively, whereas there are a few LEFPs of c1.xy, c2.xy, . . . , c8.xy. The amounts are 15, 5, 4, 2, 3, 3, 1 and 5, respectively. In the y direction, the numbers of LEFPs of k1.yx, k2.yx, . . . , k8.yx are 0, 0, 0, 0, 0, 1, 0 and 0, respectively. However, there are some LEFPs of c1.yx, c2.yx, . . . , c8.yx, whose numbers are only 15, 4, 3, 2, 1, 3, 1 and 4, respectively.

Other simulations results in which the bearing coefficients cannot be identified in some frequency intervals are obtained as follows.

(1) When the resolution is 1 nm, the coefficients of #1–3 bearing cannot be identified at 1 Hz. From 1 to 3 Hz, the coefficients of #4 and #6–8 bearing cannot be identified. From 1 to 5 Hz, the coefficients of #5 bearing cannot be identified.
(2) When the resolution is 1 um, the coefficients of #1 bearing cannot be identified from 1 to 65 Hz. From 1 to 57 Hz, the coefficients of #2 bearing cannot be identified. From 1 to 83 Hz, the coefficients of #3 bearing cannot be identified. From 1 to 99 Hz, the coefficients of #4 bearing cannot be identified. From 1 to 163 Hz, the coefficients of #5 bearing cannot be identified. From 1 to 133 Hz, the coefficients of #6 bearing cannot be identified. From 1 to 97 Hz, the coefficients of #7 bearing cannot be identified. From 1 to 107 Hz, the coefficients of #8 bearing cannot be identified.

Similar results can be obtained from simulations of g1.1 and g1.4 whose results are shown in Figures A9 and A10 in Appendix B.

According to Figure 9, the following can be obtained.

(1) 0.1 nm resolution.

Some identification errors of the main stiffness coefficients are smaller than 10%. While for the main damping coefficients, most of the identification errors are smaller than 10%.

In the x direction, the amounts of LEFPs of k1.xx, k2.xx, . . . , k8.xx are 190, 173, 106, 267, 183, 323, 142 and 166, respectively. While for c1.xx, c2.xx, . . . , c8.xx, the amounts are 900, 659, 477, 880, 954, 749, 790 and 959, respectively. In the y direction, there are 114, 73, 49, 87, 113, 250, 115 and 25 LEFPs of k1.yy, k2.yy, . . . , k8.yy, respectively. While for c1.yy, c2.yy, . . . , c8.yy, the numbers are 869, 703, 480, 925, 974, 777, 805 and 942, respectively.

As for the cross-coupled stiffness coefficients in the x direction, there are a few LEFPs of k1.xy, k2.xy, . . . , k8.xy whose numbers are 7, 58,144, 106, 73, 106, 291 and 143, respectively, whereas the amounts of LEFPs of c1.xy, c2.xy, . . . , c8.xy are 356, 689, 447, 913, 971, 594, 754 and 781, respectively. In the y direction, the numbers of LEFPs of k1.yx, k2.yx, . . . , k8.yx are 109, 127, 61, 213, 118, 184, 93 and 32, respectively. However, there are more LEFPs of c1.yx, c2.yx, . . . , c8.yx, whose numbers are 545, 751, 457, 972, 980, 678, 665 and 678, respectively.

(2) 1 um resolution.

Few identification errors of the main stiffness coefficients are smaller than 10%. While for the main damping coefficients, several identification errors are smaller than 10%.

In the x direction, the amounts of LEFPs of k1.xx, k2.xx, . . . , k8.xx are only 0, 6, 3, 1, 2, 4, 1 and 0, respectively. While for c1.xx, c2.xx, . . . , c8.xx, the amounts are 1, 46, 40, 61, 46, 60, 92 and 1, respectively. In the y direction, there are only 0, 3, 2, 0, 1, 2, 1 and 0 LEFPs of k1.yy, k2.yy, . . . , k8.yy, respectively. While for c1.yy, c2.yy, . . . , c8.yy, the numbers are 16, 41, 58, 60, 47, 109, 113 and 50, respectively.

As for the cross-coupled stiffness coefficients in the x direction, there are very few LEFPs of k1.xy, k2.xy, . . . , k8.xy whose numbers are 0, 0, 7, 0, 0, 2, 11 and 0, respectively, whereas the amounts of LEFPs of c1.xy, c2.xy, . . . , c8.xy are 356, 689, 447, 913, 971, 594, 754 and 781, respectively. In the y direction, the numbers of LEFPs of k1.yx, k2.yx, . . . , k8.yx are 0, 1, 4, 0, 1, 2, 0 and 0, respectively. However, there are several LEFPs of c1.yx, c2.yx, . . . , c8.yx, whose numbers are 0, 44, 60, 69, 52, 112, 56 and 2, respectively.

Other simulation results that the bearing coefficients cannot be identified in some frequency intervals are obtained as follows.

(1) At 1 Hz, k5.xx, k6.xx and k8.xx, c5.xx, c6.xx and c8.xx, k1.yy, k4.yy and k5.yy, c1.yy, c4.yy and c5.yy, k5.xy, k6.xy and k8.xy, c5.xy, c6.xy and c8.xy, k1.yx, k4.yx and k5.yx, c1.yx, c4.yx and c5.yx cannot be identified when the resolution is 0.1 nm.

(2) When 1 um resolution is used, k1.xx and c1.xx, k1.xy and c1.xy cannot be identified from 1 to 481 Hz and 515 to 1123 Hz. From 1 to 115 Hz, k2.xx and c2.xx, k2.xy and c2.xy cannot be identified. From 1 to 105 Hz, k3.xx and c3.xx, k3.xy and c3.xy cannot be identified. From 1 to 467 Hz, k4.xx and c4.xx, k4.xy and c4.xy cannot be identified. From 1 to 307 Hz, k5.xx and c5.xx, k5.xy and c5.xy cannot be identified. From 1 to 335 Hz, k6.xx and c6.xx, k6.xy and c6.xy cannot be identified. From 1 to 109 Hz and 121 to 249 Hz, at 859 Hz, from 863 to 865 Hz, k7.xx and c7.xx, k7.xy and c7.xy cannot be identified. From 1 to 797 Hz and 865 to 1289 Hz, k8.xx and c8.xx, k8.xy and c8.xy cannot be identified. As for the coefficients in the y direction, k1.yy and c1.yy, k1.yx and c1.yx cannot be identified from 1 to 477 Hz and 511 to 1117 Hz. From 1 to 109 Hz, k2.yy and c2.yy, k2.yx and c2.yx cannot be identified. From 1 to 101 Hz, k3.yy and c3.yy, k3.yx and c3.yx cannot be identified. From 1 to 461 Hz, k4.yy and c4.yy, k4.yx and c4.yx cannot be identified. From 1 to 301 Hz, k5.yy and c5.yy, k5.yx and c5.yx cannot be identified. From 1 to 331 Hz, k6.yy and c6.yy, k6.yx and c6.yx cannot be identified. From 1 to 115 Hz, 119 to 255 Hz, k7.yy and c7.yy, k7.yx and c7.yx cannot be identified. From 1 to 793 Hz and 869 to 1285 Hz, k8.yy and c8.yy, k8.yx and c8.yx cannot be identified.

Similar results can be obtained from simulations of h1.1 and h1.4, whose results are shown in Figures A11 and A12 in Appendix C.

3.4.2. Discussion

For Algorithm I, the following can be obtained when considering sensor resolutions.

(1) The numbers of LEFPs of the main stiffness coefficients are bigger than those of the main damping coefficients. It is indicated that the main stiffness coefficients of rolling bearings can be better identified than the main damping coefficients.

(2) The amounts of LEFPs decrease when the sensor resolution is reduced. Only several stiffness coefficients' relative errors are bigger than 10% when the sensor resolution is 0.1 nm. However, when the sensor resolution is 1 um, nearly half of the frequency points at which the stiffness coefficients' relative errors are bigger than 10% in the simulation of g4.4.

(3) When the sensor resolution is 0.1 nm, there are only dozens of, even zero LEFPs of the main stiffness coefficients in the simulation of g4.4. It is indicated that the stiffness bearing can be well identified by Algorithm I when the sensor resolution is 0.1 nm. While for the main damping coefficients, the number of LEFPs is much less than those of the main stiffness coefficients, which indicates that the stiffness coefficients cannot be well-identified. However, the damping coefficients of rolling bearings are far less than the stiffness coefficients. Hence, the damping coefficients of rolling bearings can be considered as zero. Therefore, Algorithm I can be used for rolling bearing in a multi-span and multi-disc rolling bearing-rotor system when the resolution is 0.1 nm.

As for Algorithm II used for rolling bearings, the following can be obtained.

(1) The numbers of LEFPs of the main stiffness coefficients are far greater than those of the main damping coefficients and the cross-coupled stiffness and damping coefficients. Hence, the main stiffness coefficients of rolling bearings can be better identified than the other coefficients. The reason is also that there is a very big difference between the main stiffness coefficients and the other coefficients of rolling bearings.
(2) The amounts of LEFPs decrease when the sensor resolution is reduced. In the computational example g4.4, when the sensor resolution is 0.1 nm, there is less than half of the LEFPs of the main stiffness coefficients of #3, #5 and #6 bearing. There are about seven hundred LEFPs of the main stiffness coefficients of #2, #4 and #8 bearing. There are about nine hundred LEFPs of the main stiffness coefficients of #1 and #7 bearing. When the resolution is 1 um, the number of LEFPs decreases to less than 100.

While for oil journal bearings, the following can be obtained for Algorithm II.

(1) The numbers of LEFPs of the damping coefficients of journal bearings are bigger than those of the stiffness coefficients, which indicates that the damping coefficients of journal bearings can be better identified than the stiffness coefficients.
(2) The amount of LEFPs decrease when the sensor resolution is reduced. In the computational example h4.4, when the sensor resolution is 0.1 nm, most relative errors of the damping coefficients are lower than 10%. When the sensor resolution is 1 um, the LEFPs decrease to less than 100. As for the stiffness coefficients, the number of LEFPs is much less than that of the damping coefficients. There are only several, even zero LEFPs of the stiffness coefficients in the simulation of h4.4. For journal bearings, it is necessary to identify the four stiffness coefficients and the four damping coefficients.

Therefore, the sensor resolution plays a key role when using the two algorithms. The sensor resolution affects the measured errors of the unbalance responses. Low resolution causes big measured errors. Hence, high sensor resolution is very important for improving identification accuracy. Moreover, the sensors' resolution has a considerable influence on unbalance responses at low rotating speed (frequency). This causes big measured errors of unbalance responses. Therefore, at low frequencies, the identification errors are big, and the coefficients cannot even be estimated when the resolution is low.

In addition, the identification results are improved for g1.4, g1.1,h1.4 and h1.1, in which only two bearings are included. It is indicated that the identification results will be improved when the two methods are used for simple rotors. The reason is that the solution of the inverse matrix of H_1 and H_3 in the two algorithms is more accurate when the algorithms are used for simple rotors g1.4, g1.1, h1.4 and h1.1. When the two algorithms are used for complex rotors, the inverse matrix of H_1 and H_3 may be inaccurate and they might not even be solved where the measured errors of unbalance responses are too big, which is caused by low resolution.

4. Conclusions

In this paper, two novel algorithms are proposed to estimate each bearings' coefficients of a multi-disc and multi-span rotor using unbalance responses. Numerical simulations are conducted to study the proposed algorithms and the results are summarized as follows.

(1) The proposed algorithms provide a technique by which the stiffness and damping coefficients of each bearing can be monitored online under operation conditions. To identify the coefficients of all bearings in a rotor with n bearings and m discs, there should be m + n + 1 measured unbalance responses in both x and y directions. Moreover, the unbalance responses of each bearing should be measured. Algorithm I is suitable for rolling bearing coefficient identification, while Algorithm II can be applied to estimating both rolling-bearing coefficients and oil-journal bearing coefficients. External excitations and test runs are not required for the two algorithms. However, it is necessary to change the rotating speed slightly when using Algorithm II.

(2) Adjustment points play a critical role in improving the identification accuracy of the two algorithms. Numerical simulations indicate that the coefficients of the bearing, which the adjustment point is near, are accurately identified. While the identification errors of the bearing, from which the adjustment point is far away, are often very big. Hence, in order to identify all bearings' coefficients accurately, there should be an adjustment point near each bearing.

(3) Accuracy of the unbalance response measurement system is very important to the two algorithms. Numerical simulations indicate that if the measuring errors of all the required unbalance responses are zero or the same, the identification errors are almost equal to zero. It is indicated that the repeatability precision of each measuring channel of the unbalance response measurement system plays a key role when using the two algorithms. Moreover, the two algorithms require high sensor resolution. The sensor resolution is higher, and the estimation accuracy is higher. Sensors with a resolution of 1 um should be avoided and sensors with a resolution of 0.1 nm are recommended for practical application.

For further study, experimental investigations should be organized to prove the proposed methods. The continuous model of the rotor can be developed based on Timoshenko theory because gyroscopic moments are considered. The limitation of the proposed algorithms is that high accuracy of the measurement of unbalance responses is strongly demanded. The research method of this paper can be regarded as a tool for future study.

Author Contributions: Conceptualization, A.W.; methodology, A.W.; software, A.W., Y.B., Y.X. and Y.F.; formal analysis, A.W.; investigation, Y.X., X.C. and J.Y.; writing—original draft preparation, A.W. and Y.B.; writing—review and editing, A.W. and Y.B.; supervision, G.M.; funding acquisition, G.M. All authors have read and agreed to the published version of the manuscript.

Funding: This research was funded by the Fundamental Research Funds for the Central Universities, grant number 8000150A084 and the Yue Qi Scholar Project, China University of Mining & Technology, Beijing, grant number 800015Z1145.

Institutional Review Board Statement: Not applicable.

Informed Consent Statement: Not applicable.

Data Availability Statement: The study did not report any data.

Conflicts of Interest: The authors declare no conflict of interest.

Appendix A

(1) Simulation of g1.4.

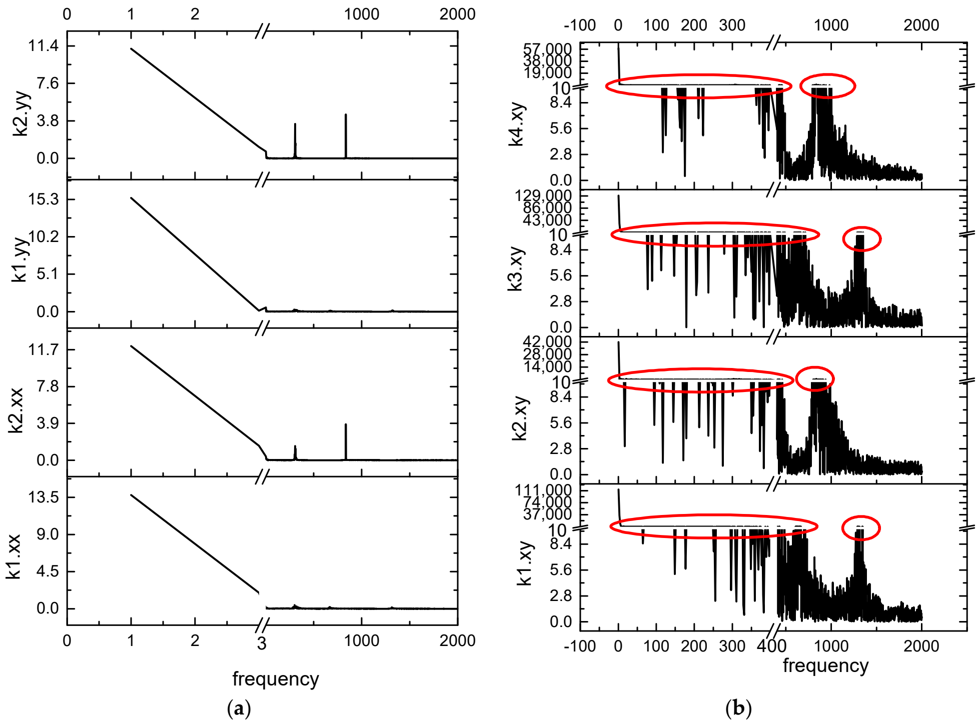

Figure A1. Identified bearing coefficients changing with frequency of g1.4 based on Algorithm I considering adjustment point and sensor resolution 1a: (a) obtained main stiffness coefficients in x and y directions from 0 to 2000 Hz; (b) obtained main damping coefficients in x and y directions.

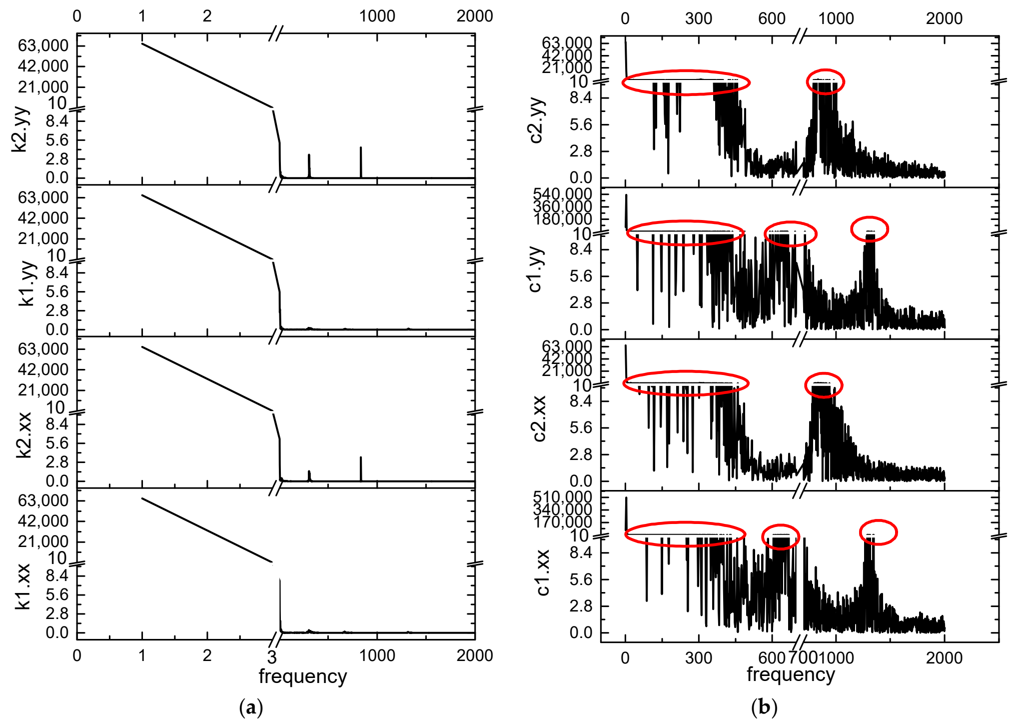

Figure A2. Identified bearing coefficients changing with frequency of g4.4 based on Algorithm I considering adjustment point and sensor resolution 1 nm: (a) obtained main stiffness coefficients in x and y directions; (b) obtained main damping coefficients in x and y directions.

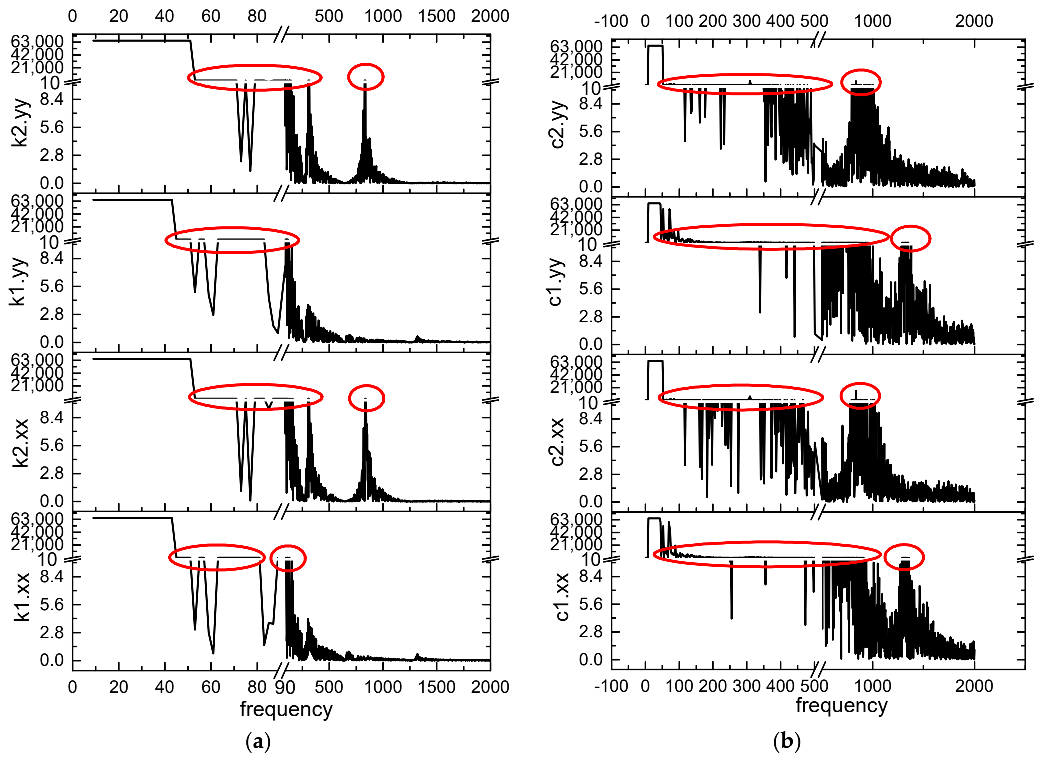

Figure A3. Identified bearing coefficients changing with frequency of g1.4 based on algorithm I considering adjustment point and sensor resolution 1 um: (**a**) obtained main stiffness coefficients in x and y directions; (**b**) obtained main damping coefficients in x and y directions.

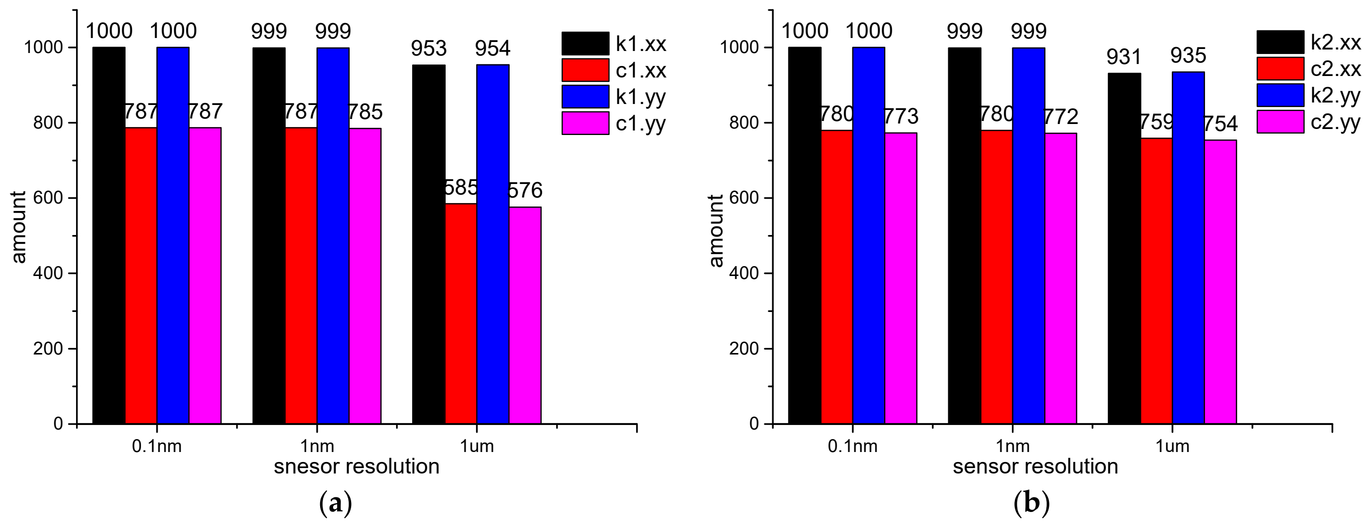

Figure A4. Statistical results of the amount of the frequencies, at which the related error is less than 10%: (**a**) #1 bearing; (**b**) #2 bearing.

(2) Simulation of g1.1.

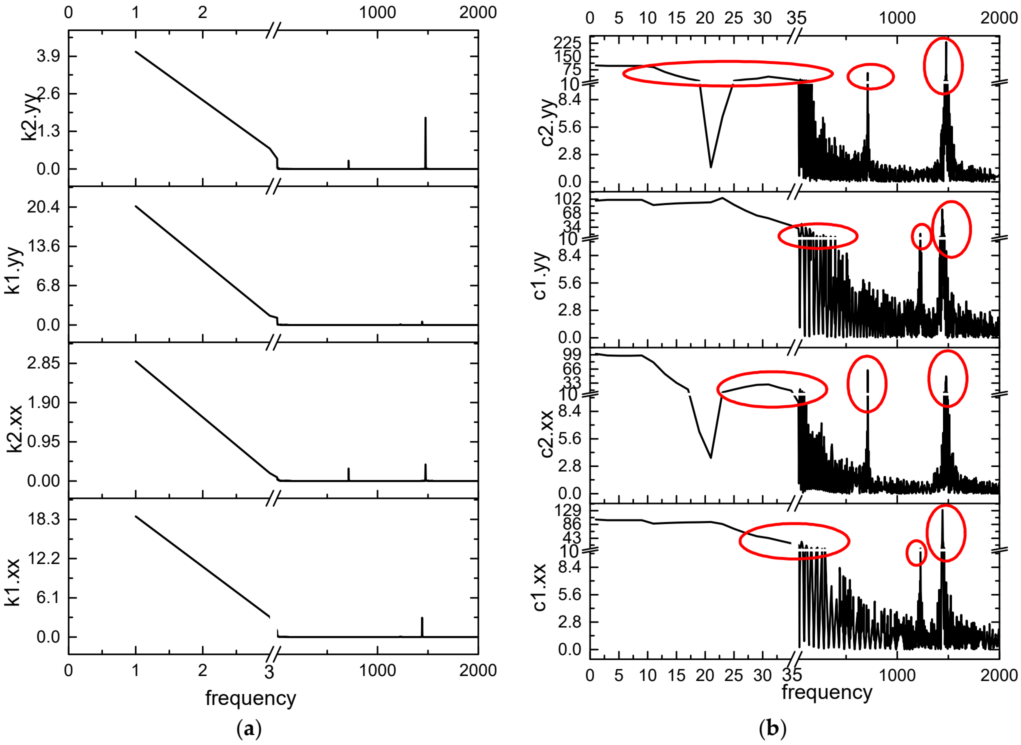

Figure A5. Identified bearing coefficients changing with frequency of g1.1 based on algorithm I considering adjustment point and sensor resolution 1 am: (**a**) obtained main stiffness coefficients in x and y directions; (**b**) obtained main damping coefficients in x and y directions.

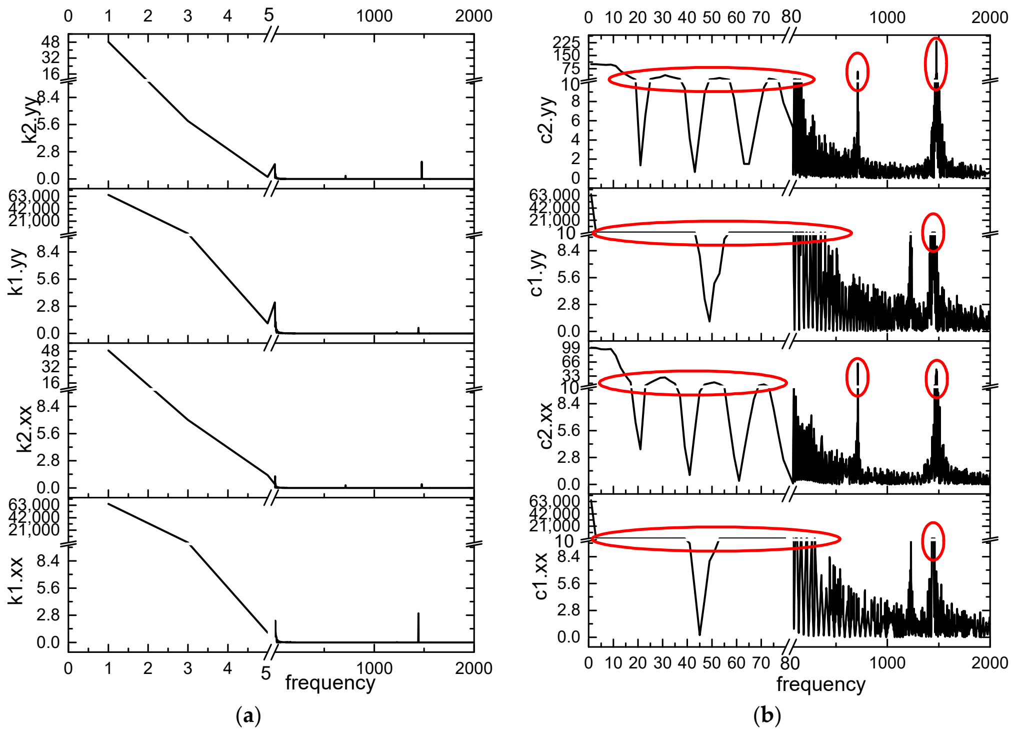

Figure A6. Identified bearing coefficients changing with frequency of g1.1 based on algorithm I considering adjustment point and sensor resolution 1 nm: (**a**) obtained main stiffness coefficients in x and y directions; (**b**) obtained main damping coefficients in x and y directions.

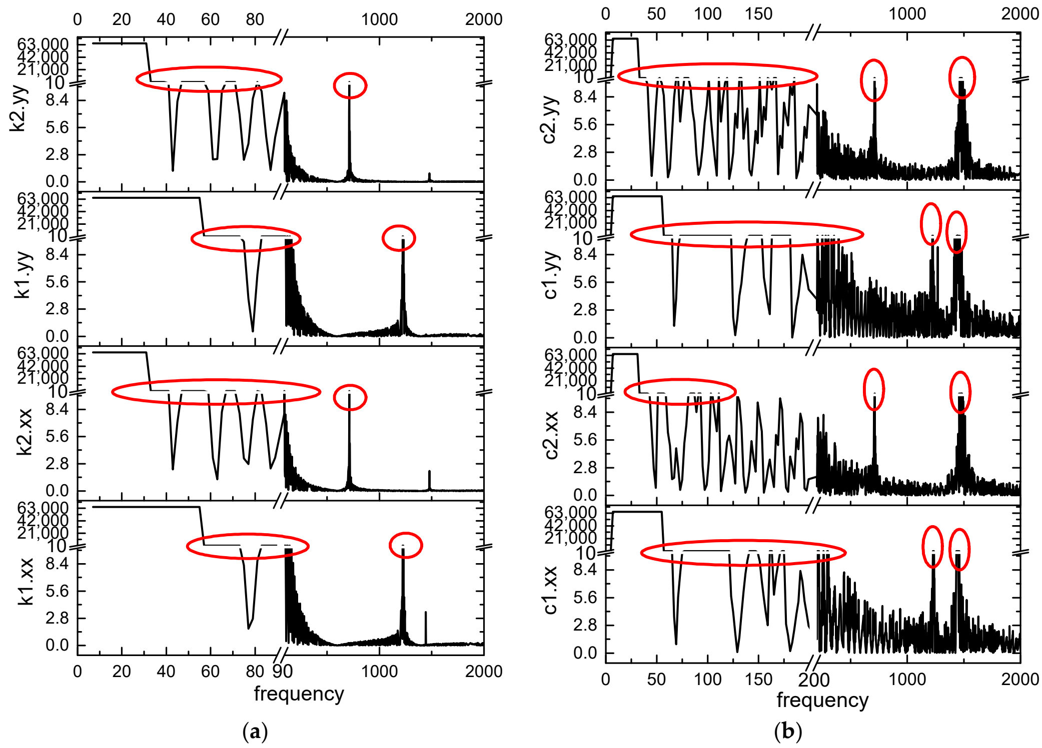

Figure A7. Identified bearing coefficients changing with frequency of g1.1 based on algorithm I considering adjustment point and sensor resolution 1 um: (**a**) obtained main stiffness coefficients in x and y directions; (**b**) obtained main damping coefficients in x and y directions.

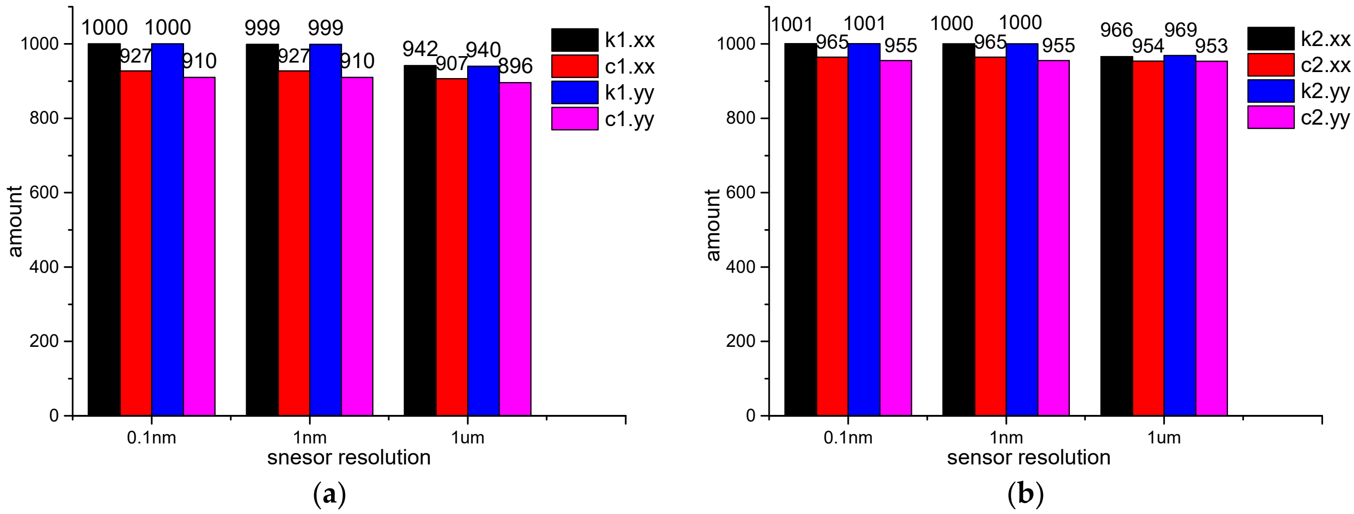

Figure A8. Statistical results of the amount of the frequencies, at which the related error is less than 10%: (**a**) #1 bearing; (**b**) #2 bearing.

Appendix B

(1) Simulation of g1.4.

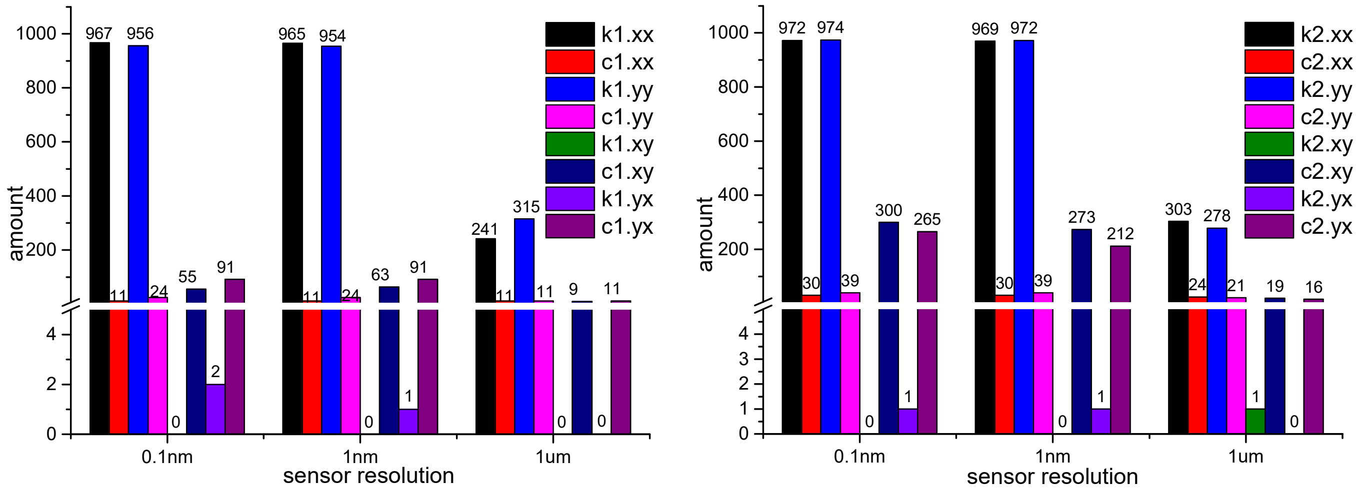

(a) (b)

Figure A9. Statistical results of the amount of the frequencies, at which the related error is less than 10% and the absolute value is less than 10: (**a**) #1 bearing; (**b**) #2 bearing.

(2) Simulation of g1.1.

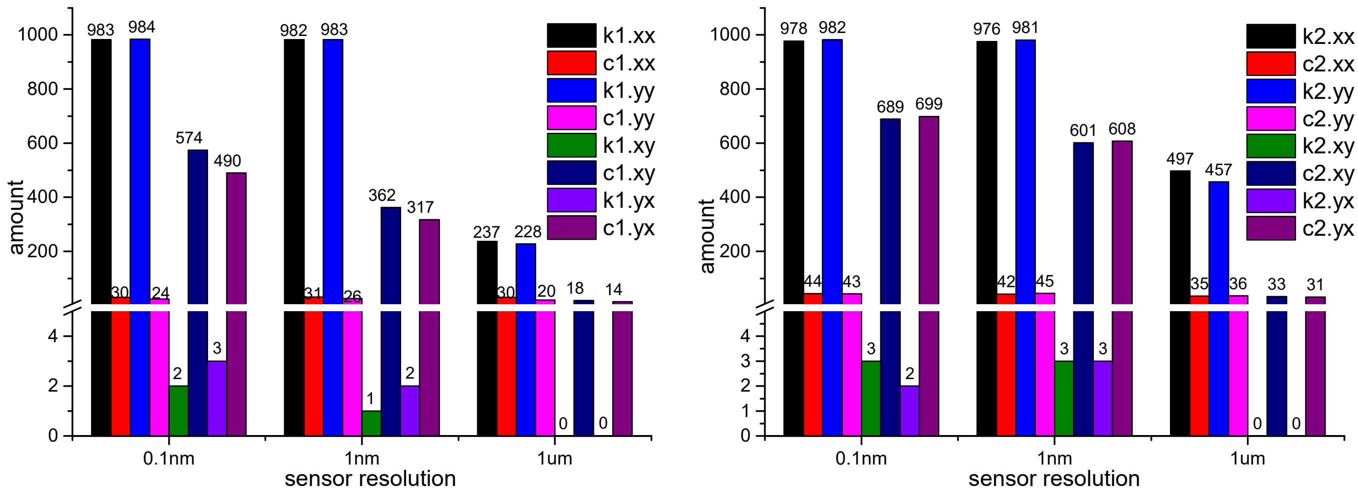

(a) (b)

Figure A10. Statistical results of the amount of the frequencies, at which the related error is less than 10% and the absolute value is less than 10: (**a**) #1 bearing; (**b**) #2 bearing.

Appendix C

(1) Simulation of h1.4.

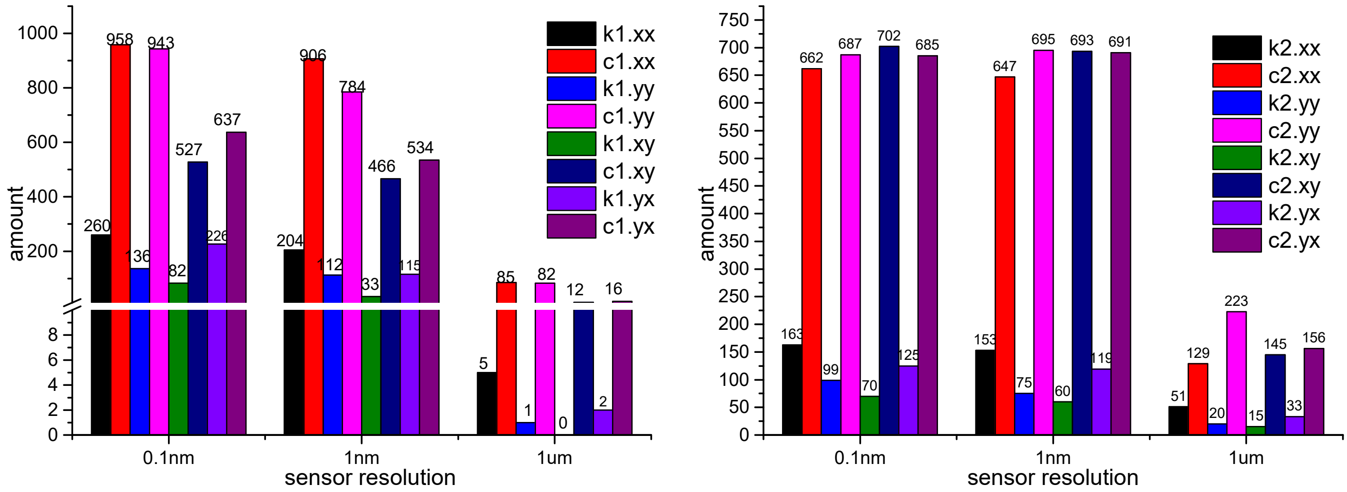

(**a**) (**b**)

Figure A11. Statistical results of the amount of the frequencies, at which the related error is less than 10% and the absolute value is less than 10: (**a**) #1 bearing; (**b**) #2 bearing.

(2) Simulation of h1.1

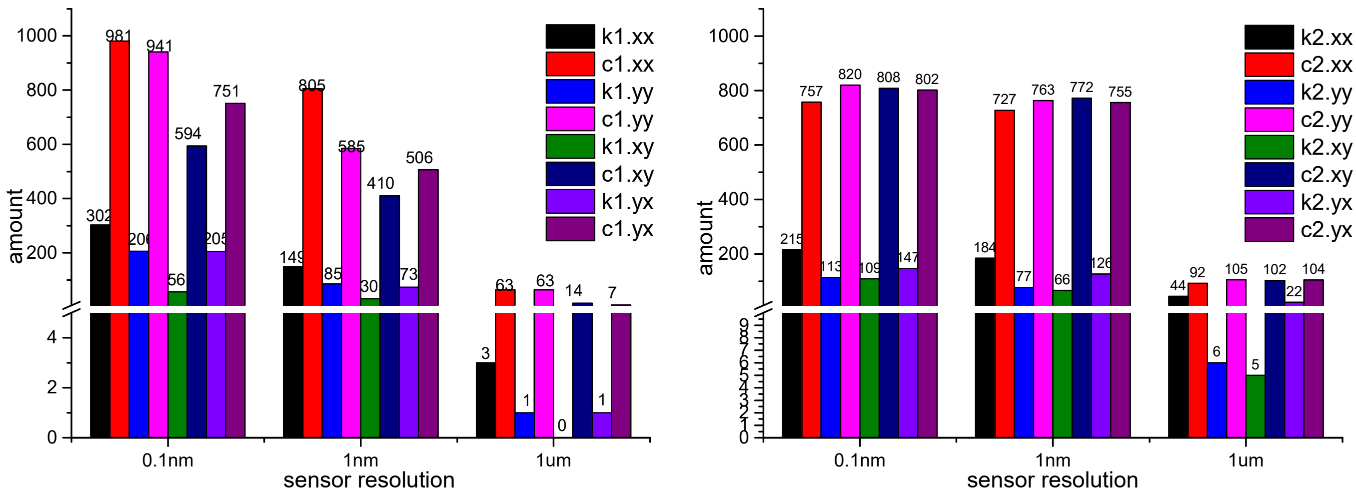

(**a**) (**b**)

Figure A12. Statistical results of the amount of the frequencies, at which the related error is less than 10% and the absolute value is less than 10: (**a**) #1 bearing; (**b**) #2 bearing.

References

1. Chen, W. A Simplified Identification Method of Dynamic Stiffness for the Heavy-Load and Low-Speed Journal Bearings. *Teh. Vjesn.* **2020**, *27*, 125–132.
2. Kim, S.H.; Yeon, S.M.; Lee, J.H.; Kim, Y.W.; Lee, H.; Park, J. Additive manufacturing of a shift block via laser powder bed fusion: The simultaneous utilisation of optimised topology and a lattice structure. *Virtual Phys. Prototyp.* **2020**, *15*, 460–480. [CrossRef]
3. Snyder, T.; Braun, M. Comparison of perturbed reynolds equation and cfd models for the prediction of dynamic coefficients of sliding bearings. *Lubricants* **2018**, *6*, 5. [CrossRef]
4. Li, Q.; Zhang, S.; Ma, L.; Xu, W.; Zheng, S. Stiffness and damping coefficients for journal bearing using the 3D transient flow calculation. *J. Mech. Sci. Technol.* **2017**, *31*, 2083–2091. [CrossRef]
5. Dyk, Š.; Rendl, J.; Byrtus, M.; Smolík, L. Dynamic coefficients and stability analysis of finite-length journal bearings considering approximate analytical solutions of the Reynolds equation. *Tribol. Int.* **2019**, *130*, 229–244. [CrossRef]
6. Merelli, C.E.; Barilá, D.O.; Vignolo, G.G.; Quinzani, L.M. Dynamic coefficients of finite length journal bearing. Evaluation using a regular perturbation method. *Int. J. Mech. Sci.* **2019**, *151*, 251–262. [CrossRef]

7. Kang, Y.; Shi, Z.; Zhang, H.; Zhen, D.; Gu, F. A novel method for the dynamic coefficients identification of journal bearings using Kalman filter. *Sensors* **2020**, *20*, 565. [CrossRef]
8. Li, Q.; Wang, W.; Weaver, B.; Wood, H. Model-based interpolation-iteration method for bearing coefficients identification of operating flexible rotor-bearing system. *Int. J. Mech. Sci.* **2017**, *131*, 471–479. [CrossRef]
9. Tiwari, R.; Lees, A.W.; Friswell, M.I. Identification of dynamic bearing parameters: A review. *Shock. Vib. Dig.* **2004**, *36*, 99–124. [CrossRef]
10. Mutra, R.R. Identification of rotor bearing parameters using vibration response data in a turbocharger rotor. *J. Comput. Appl. Res. Mech. Eng.* **2019**, *9*, 145–156.
11. Hagg, A.C.; Sankey, G.O. Some dynamic properties of oil-film journal bearings with reference to the unbalance vibration of rotors. *J. Appl. Mech.* **1956**, *78*, 302–306. [CrossRef]
12. Duffin, S.; Johnson, B.T. Paper 4: Some Experimental and Theoretical Studies of Journal Bearings for Large Turbine-Generator Sets. In Proceedings of the Institution of Mechanical Engineers, London, UK, 1 June 1966.
13. Tiwari, R.; Lees, A.W.; Friswell, M.I. Identification of speed-dependent bearing parameters. *J. Sound Vib.* **2002**, *254*, 967–986. [CrossRef]
14. Tyminski, N.C.; Tuckmantel, F.W.; Cavalca, K.L.; de Castro, H.F. Bayesian inference applied to journal bearing parameter identification. *J. Braz. Soc. Mech. Sci. Eng.* **2017**, *39*, 2983–3004. [CrossRef]
15. Chen, C.; Jing, J.; Cong, J.; Dai, Z. Identification of dynamic coefficients in circular journal bearings from unbalance response and complementary equations. *Proc. Inst. Mech. Eng. Part J J. Eng. Tribol.* **2019**, *233*, 1016–1028. [CrossRef]
16. Song, Q.; Sun, F.; Ma, J. A New Algorithm and Experimental Investigation for the Identification of Dynamic Characteristics of Journal Bearings. *J. Beijing Inst. Technol.* **2002**, *22*, 682–686.
17. Tiwari, R.; Chakravarthy, V. Identification of the bearing and unbalance parameters from rundown data of rotors. In *IUTAM Symposium on Emerging Trends in Rotor Dynamics*; Springer: Dordrecht, The Netherlands, 2011.
18. Bently, D.E. Modal testing and parameter identification of rotating shaft/fluid lubricated bearing system. In Proceedings of the Fourth International Conference on Modal Analysis, Los Angeles, CA, USA, 3–6 February 1986.
19. Stanway, R.; Tee, T.K.; Mottershead, J.E. Identification of squeeze-film bearing dynamics using a recursive, frequency-domain filter. In Proceedings of the ASME Twelfth Biennial Conference on Mechanical Vibration and Noise, Montreal, QC, Canada, 17–21 September 1989.
20. Iida, H. Application of the Experimental Determination of Character Matrics to the Balancing of a Flexible Rotor. In Proceedings of the IFToMM 4th International Conference on Rotor Dynamics, Chicago, IL, USA, September 1994.
21. Tiwari, R. Chakravarthy, V. Simultaneous identification of residual unbalances and bearing dynamic parameters from impulse responses of rotor–bearing systems. *Mech. Syst. Signal Processing* **2006**, *20*, 1590–1614. [CrossRef]
22. Tiwari, R.; Chakravarthy, V. Simultaneous estimation of the residual unbalance and bearing dynamic parameters from the experimental data in a rotor-bearing system. *Mech. Mach. Theory* **2009**, *44*, 792–812. [CrossRef]
23. Tiwari, R. Conditioning of regression matrices for simultaneous estimation of the residual unbalance and bearing dynamic parameters. *Mech. Syst. Signal Processing* **2005**, *19*, 1082–1095. [CrossRef]
24. Wang, A.; Yao, W.; He, K.; Meng, G.; Cheng, X.; Yang, J. Analytical modelling and numerical experiment for simultaneous identification of unbalance and rolling-bearing coefficients of the continuous single-disc and single-span rotor-bearing system with Rayleigh beam model. *Mech. Syst. Signal Processing* **2019**, *116*, 322–346. [CrossRef]
25. Wang, A.; Xia, Y.; Cheng, X.; Yang, J.; Meng, G. Continuous Rotor Dynamics of Multi-disc and Multi-span Rotor: Theoretical and Numerical Investigation on Continuous Model and Analytical Solution for Unbalance Responses. *Appl. Sci.* **2022**. *accepted*.
26. Wang, A.; Feng, Y.; Yang, J.; Cheng, X.; Meng, G. Continuous Rotor Dynamics of Multi-disc and Multi-span Rotor: A Theoretical and Numerical Investigation on Identification of Rotor Unbalance from Unbalance Responses. *Appl. Sci.* **2022**, *12*, 3865. [CrossRef]
27. Wang, A.; Yao, W. Theoretical and Numerical Studies on Simultaneous Identification of Rotor Unbalance and Sixteen Dynamic Coefficients of Two Bearings Considering Unbalance Responses. *Int. J. Control. Autom. Systems* 2021, *accepted*.